

FINAL REPORT

DETECTION AND MITIGATION OF SUBSIDENCE AND VOIDS ON VERMONT ROADWAYS

I-89 Hartford and US 7 Manchester, Vermont

May 30, 2008

*Contract No. 0984747
ARA Project No. 17986*

*Prepared for:
Vermont Agency of Transportation
Montpelier, VT*

*Prepared by:
Applied Research Associates, Inc.
461 Waterman Road
South Royalton, VT 05068*

“The information contained in this report was compiled for the use of the Vermont Agency of Transportation. Conclusions and recommendations contained herein are based upon the research data obtained and the expertise of the researchers, and are not necessarily to be construed as Agency policy. This report does not constitute a standard, specification, or regulation. The Vermont Agency of Transportation assumes no liability for its contents or the use thereof.”

1. Report No. 2008-7	2. Government Accession No.	3. Recipient's Catalog No.	
4. Title and Subtitle DETECTION AND MITIGATION OF SUBSIDENCE AND VOIDS ON VERMONT ROADWAYS: I-89 Hartford and US 7 Manchester, Vermont		5. Report Date May 2008	
		6. Performing Organization Code	
7. Author(s) Applied Research Associates, Inc.		8. Performing Organization Report No.	
9. Performing Organization Name and Address Applied Research Associates, Inc. 461 Waterman Road South Royalton, VT 05068		10. Work Unit No.	
		11. Contract or Grant No. 0984747	
12. Sponsoring Agency Name and Address Vermont Agency of Transportation Materials and Research Section National Life Building Montpelier, VT 05633-5001		13. Type of Report and Period Covered	
		14. Sponsoring Agency Code	
15. Supplementary Notes			
16. Abstract <p>During the summer of 2007, a geophysical survey team from Applied Research Associates, Inc. evaluated two Vermont highway sites exhibiting subsidence. We performed surveys on I-89 in Hartford and on US-7 in Manchester to assess the performance of three non-destructive geophysical methods for characterizing the causes of subsidence. Using a set of performance criteria, we selected three non-invasive geophysical methods for field evaluations at the two subsidence sites. Our objectives for these field trials were to identify the causes of subsidence as well as determine the effectiveness and feasibility of employing these methods for characterizing the subsidence conditions.</p> <p>Subsidence at both sites is likely resulting from a combination of drainage issues and construction processes. The methods we employed proved effective for characterizing subsurface conditions at the two sites, including CPT to verify the relative soil strength conditions. Additionally, these methods may prove viable for future investigative applications such as wide area assessments and network level surveys.</p>			
17. Key Words subsidence, voids, non-destructive testing		18. Distribution Statement	
19. Security Classif. (of this report)	20. Security Classif. (of this page)	21. No. Pages 28	22. Price

Executive Summary

During the summer of 2007, a geophysical survey team from Applied Research Associates, Inc. evaluated two Vermont highway sites exhibiting subsidence. We performed surveys on I-89 in Hartford and on US-7 in Manchester to assess the performance of three non-destructive geophysical methods for characterizing the causes of subsidence. The sites offered significantly different conditions; the original pavement structure at the Hartford site had been modified by years of patching while the Manchester site maintained the original structure. Using a set of performance criteria, we selected three non-invasive geophysical methods for field evaluations at the two subsidence sites. Our objectives for these field trials were to identify the causes of subsidence as well as determine the effectiveness and feasibility of employing these methods for characterizing the subsidence conditions. We used Ground Penetrating Radar (GPR), Capacitively Coupled Resistivity (CCR), Falling Weight Deflectometry (FWD) and Cone Penetrometry (CPT) to investigate the underlying structural health of the roadways. Prior to the surveys, the potential existence of large voids or cavities beneath the sites was of primary concern to VTrans; however, analysis of data collected at the sites did not indicate the presence of any possibly catastrophic anomalies. Subsidence at both sites is likely resulting from a combination of drainage issues and construction processes. The Hartford site shows signs of insufficient surface drainage control that has likely caused a slow migration of fines from the base material, leaving small but pervasive voids or low-density regions. Subsidence at the Manchester site may be due to a non-uniformly compacted base that demonstrates a weak material at depths greater than 13 ft. Insight gained from geophysical data analysis combined with information about the site histories proved valuable for assessing the structural health and characterizing the subsidence conditions. The methods we employed proved effective for characterizing subsurface conditions at the two sites, including CPT to verify the relative soil strength conditions. Additionally, these methods may prove viable for future investigative applications such as wide area assessments and network level surveys.

Preface

This report was prepared by Jonathan Miller, Dr. Gregory Schultz and Darryl Calkins, Applied Research Associates Inc., 461 Waterman Road, South Royalton, VT under contract with the Vermont Agency of Transportation, No. 0984747. The authors would like to acknowledge the assistance provided to us from several staff members in the Agency of Transportation. They are Chris Benda, Tammy Ellis, Trevor Starr and Nelson Blanchard as well as Jim Raymond who operated the FWD and members of the drilling/coring unit that provided support on drilling through the pavement at both sites. The authors also thank Dr. Steven Arcone, US Army Cold Regions Research & Engineering Laboratory for his support, advice and interpretation of GPR data.

Table of Contents

Executive Summary	i
Preface.....	i
Table of Contents.....	ii
List of Figures.....	ii
List of Tables	iii
1 Introduction.....	1
2 Background.....	1
3 Methods.....	1
3.1 Geophysical.....	1
3.2 Mitigation.....	3
4 Advanced Selection	4
4.1 GPR.....	4
4.2 CCR.....	5
4.3 FWD.....	5
4.4 Other Methods	6
5 Site Description.....	6
5.1 I-89 Hartford.....	6
5.2 US-7 Manchester	8
6 Data Collection	9
6.1 Equipment.....	9
GPR.....	9
CCR.....	9
FWD.....	9
CPT	10
6.2 Techniques	10
GPR:.....	10
CCR:	10
FWD:.....	11
CPT:	11
7 Site Specific Analysis	11
7.1 I-89 Hartford.....	11
7.2 US-7 Manchester	13
8 Results.....	15
8.1 I-89.....	15
8.2 US-7	19
9 Conclusions and Recommendations	24
9.1 Method Selection	24
9.2 Protocol.....	25
9.3 Mitigation.....	27

List of Figures

Figure 5.1 Interstate 89 survey site.....	7
-------------------------------------------	---

Figure 5.2 Interstate 89, Hartford, Vermont looking east toward New Hampshire. The asphalt patch extending across both southbound lanes indicates the region of subsidence..... 8

Figure 5.3 US 7 survey site..... 8

Figure 5.4 (a) Photograph of US Route 7, Manchester, Vermont looking north. Two dips formed across both lanes. (b) Elevation profile map of dips. Dotted lines indicate surveyed points. 9

Figure 6.1 (a) GSSI cart-mounted GPR. (b) Geometrics OhmMapper CCR towed array. (c) Dynatest® FWD trailer system. 10

Figure 6.2 Layout of parallel GPR survey transects at I-89 site. Parallel transects were spaced at 3.28 ft intervals. Across-road transects (not shown) were spaced at 6.6 ft intervals. 10

Figure 6.3 Layout of parallel CCR survey transects at US-7 site. Transects were spaced at roughly 6.6 ft intervals..... 11

Figure 7.1 400-MHz GPR data beginning at stationing 131+22. Clusters of small reflectors are shown beneath the asphalt patch. 12

Figure 7.2 Apparent resistivity profile. The asphalt patch is the dominant feature in this pseudosection. The regions of high resistivity (red) correspond to asphalt layers..... 12

Figure 7.3 Deflection values generated from RWD (blue) measurements and FWD (red) measurements. 13

Figure 7.4 Correlated GPR and CCR data. Dotted red lines correspond to subsidence zone. GPR data are “washed out” due to attenuation in this region. The solid red line is the original ground elevation at the site. The dotted blue line traces the subgrade layer shown in the GPR profile..... 14

Figure 7.5 FWD deflection profiles show increased values over dips. Deflection peaks correspond to surface cracks close to the dips..... 14

Figure 7.6 Layer modulus profiles. The subgrade modulus increases just after the dip locations. 15

Figure 8.1 Full CPT sounding, test #4. 16

Figure 8.2 Segment of CPT sounding, test #4. 17

Figure 8.3 Segment of CPT sounding, test #5. 17

Figure 8.4 (a) CPT profiles. Drops in blow count and tip pressure (blue and green respectively) and spikes in sleeve/tip ratio (red) indicate voids. (b) Borehole showing subbase composition. (c) Sinkhole near the site. 18

Figure 8.5 Correlation of GPR and CCR data reveal regions of saturation beneath the subsidence zones (dips). The high modulus subgrade (dark blue) corresponds to a compacted base layer that appears to retain water into the saturated zones..... 19

Figure 8.6 400 MHz radar plot with CPT locations..... 20

Figure 8.7 200 MHz radar plot with CPT sounding locations..... 20

Figure 8.8 CPT sounding at site 5 which is the middle crest between the two dips..... 21

Figure 8.9 CPT sounding at site 8, on the outer crest of dip #2..... 22

Figure 8.10 400 MHz GPR transect overlaid with CPT tip pressure traces. 22

Figure 8.11 Correlation between GPR profile (left) and CPT profile (right). Yellow and blue layers correspond to dynamically compacted fill layers; the red layer corresponds to the original ground layer..... 23

List of Tables

Table 1: Considered methods and total score based on weighted selection criteria. Yellow indicates methods selected for field testing. Blue indicates ground-truth methods..... 2

Table 2 Generic mitigation matrix..... 4

Table 3: CPT locations, I-89 Southbound Lane, 23 August 2007	15
Table 4 CPT locations-US-7 Northbound Lane: Data taken at 3.3 feet off centerline	20
Table 5 Evaluation matrix for US-7 subsidence	24

1 Introduction

Road subsidence indicates a failing or insufficient pavement substructure. The pervasive nature of subsidence throughout the country's aging highway infrastructure makes full-scale reconstruction of every site costly and often infeasible. A variety of conditions can lead to subsidence. Some processes, such as large void formation, may lead to sudden and catastrophic pavement failure; while other processes, such as slow migration of fine particles from the sub base, may cause gradual or seasonal subsidence. Assessing the potential for catastrophic failure of subsiding roads is critical to determining the extent and timeliness of the remediation required. Noninvasive geophysical and non-destructive testing (NDT) methods provide cost efficient alternatives to interpolating borehole data used to characterize roadway subsidence and map subsurface voids. In this study we present the results from data collected at two Vermont highway sites exhibiting pavement subsidence. We employed complementary nondestructive methods to locate subsurface voids or conditions that cause subsidence. High-resolution ground penetrating radar (GPR) grid sampling combined with capacitively-coupled resistivity (CCR) surveying over the locations of subsidence elucidated the causes of the failing pavement substructure. Spatially correlated GPR and CCR cross-sections were combined with falling weight deflectometer (FWD) test results to refine our interpretations and guide direct investigations with a cone penetrometer. Our results indicate that the conditions of the site, specifically those resulting from interim repairs, can have a large impact on the effectiveness of these methods.

2 Background

The state of Vermont owns and maintains over 1100 large culverts (> 6 feet in diameter) on Interstate and State highways. The vast majority of these are between 30 and 50 years old. In June 2003, a culvert in this same age range on Interstate 70 west of Denver, Colorado failed due to rusting and created a large sinkhole, blocking four lanes and causing a 2-hour delay. After four days, two lanes were temporarily re-opened. The final repair of the 90 foot long culvert was completed after 49 days and \$4.2 million (Perrin, 2004).

Although subsidence and voids may be caused by a number of processes, subsidence associated with the failure of culverts and other highway infrastructure cause sudden and often dangerous hazards. As exemplified by the \$1.1 million replacement of a culvert under I-89 in Rockingham, the repair of large culverts on Vermont highways can be expensive and disruptive to traffic. Through early detection/characterization and mitigation of roadway subsidence and voids, VTrans may be able to avoid the hazards and costs of catastrophic failures such as those in Colorado and other states.

3 Methods

3.1 Geophysical

Geophysical and NDT data are often acquired in a sequential fashion, where lower-resolution higher-speed acquisition approaches used for reconnaissance and detection are followed by more focused higher-resolution evaluations to provide verification and more detailed characterization information to support decisions about remediation strategies (Bouillon, 2005). Characterization of subsidence conditions requires sensing methods that provide high resolution measurement of

geophysical parameters such as soil density, dielectric permittivity, and conductivity. Several nondestructive or minimally invasive techniques exist that can establish these properties for the pavement substructure. While field testing all of these methods at a subsidence location would provide a comprehensive performance evaluation of each method, we downselected three methods to minimize project costs and comply with the objective of defining a feasible site assessment protocol.

To quantify the selection process, we used four principal criteria to identify appropriate geophysical methods for testing:

1. *Effectiveness* – general technology maturity, success in similar applications, application-relevant attributes (i.e., effectiveness in detecting voids or subsurface anomalies)
2. *Feasibility* – operational costs/constraints, transportability and availability, environmental limitations (e.g., performance degradation in wet conditions)
3. *Invasiveness* – extent of damage to pavement/base, costs for damage repair (including repair downtime)
4. *Efficiency* – rate of coverage, spatial sampling resolution

We weighted these criteria to reflect the contribution of each to the overall evaluation. While applying weighting values to the criteria was subjective, it was an attempt to quantify a difficult and often completely qualitative decision making process. Table 1 lists the considered methods and their weighted scores. Applicability of the methods to each criterion is based on a scale of 0 to 3 (0-not applicable, 3-highly applicable); the total score reflects the weighted sum of each criterion.

Table 1: Considered methods and total score based on weighted selection criteria. Yellow indicates methods selected for field testing. Blue indicates ground-truth methods.

Method	Effectiveness (0.4)	Feasibility (0.2)	Invasiveness (0.2)	Efficiency (0.2)	Total
Ground Penetrating Radar	3	2	3	3	2.8
AC Resistivity	3	2	3	3	2.8
Falling Weight Deflectometer	3	2	3	2	2.6
Surface Wave Seismics	3	2	2	2	2.4
Seismic Reflection	2	3	2	1	2
Seismic Refraction	2	3	2	1	2
Electromagnetic Induction	1	2	3	3	2
Infrared Imaging	1	2	3	3	2
Cross-hole Seismic Tomography	3	2	1	1	2
Electrical Resistance Tomography	3	2	1	1	2
Cross-hole Radar	3	2	1	1	2
Gravity	2	2	3	1	2
Cone Penetrometer Testing	3	1	0	1	1.6
Boring, Drilling, and Excavation	3	1	0	1	1.6

Evaluation of methods for use in particular applications should factor in project-specific constraints, such as 1) conditions of the site, 2) time, funds, and computational resources available for an

investigation, 3) experience of the investigator, and 4) availability of supporting data. Applying our project-specific constraints to the selection criteria yielded three high-scoring methods: Ground Penetrating Radar (GPR), AC (or Capacitively-Coupled) Resistivity (CCR), and Falling Weight Deflectometer (FWD). We also selected two invasive methods (Cone Penetrometer Testing and Boring) for selective ground-truthing.

While all of the methods listed in Table 1 are widely accepted as effective subsurface geophysical characterization techniques, we down-selected to three methods by applying our four evaluation metrics. We assessed the effectiveness of the various methods primarily through extensive literature reviews. Studies that reveal the successes or failures of specific methods are a valuable resource for gauging the capabilities of these techniques in similar applications. We compiled several sources that cited studies where non-destructive geophysical technologies were employed for void detection and characterization of subsurface anomalies. We applied the other metrics (feasibility, invasiveness, and efficiency) to assess the general operational capabilities and limitations of each method. Section 4 describes our advanced selection process and elaborates on, for the three chosen methods, the attributes relevant to each metric.

3.2 Mitigation

The process of identifying the mitigation technique starts with clearly understanding the processes involved in the subsidence and the underlying mechanics. We will assume that subsidence occurs by the translocation of soil particles such that voids occur or the particle to particle forces change, both resulting in downward vertical displacement of material above the failure zone. Each subsidence problem will likely be unique, but general categories did emerge in the review of the literature.

The main categories are as follows in which voids are created in the soils

1. Failure of conveyance structures beneath the highway section
 - a. Corrosion in metallic culverts
 - b. Structural failure of the structure
 - c. Invert “wear-through” in culverts
 - d. Subsurface flow beneath culverts
2. Soil material failures and their movement in the base & subbase
 - a. Excessive stresses from roadway traffic
 - b. Infiltration of water and subsequent particle dislodgement & movement

The mitigation techniques are limited and generally can be grouped into three categories.

1. Surface treatment:
 - i. Pavement trimming & hot mix overlays
 - ii. Surface drainage controls
2. In-situ soil strength treatments: Grouting
 - i. Low pressure
 - a. Compaction
 - b. Cement
 - c. Fracture
 - ii. High pressure
 - a. Single fluid systems
 - b. Multi fluid systems
 - iii. Chemical
3. Replacement of complete highway section,
 - i. Soil replacements

ii. Non native structural components

For example, if the voids are located just below the concrete or asphalt pavement, then shallow depth injection of an additive (chemical/cement) can be achieved by augering holes through the pavement surface and then inserting the injection tube to the required depth; however, at deeper depths coring, followed by hole stabilization may be required before the injection tube can be inserted.

The problem sites will always be different and the highway conditions will also vary. For example, a rural 2 lane versus a multi-lane one way traffic stream is significantly different from a structural viewpoint to a safety concern for workers; hence it is difficult to generalize mitigation alternatives for such a wide range of conditions. It is our recommendation that each site go through a matrix of alternatives.

A generic matrix of assessment could be as follows for a 2 lane highway with very long sight distances and treatment depth 10-15 feet below the pavement surface. The categories are assessed in terms of low, medium and high.

Table 2 Generic mitigation matrix

Mitigation Technique	Probability of Success	Disruption to Traffic	Contractor Availability	Q/A & Durability	Safety of Operations	Costs
Surface Treatments	Low-Med	Low	High	Low	High	Low
In-situ soil strength treatments	Med-High	Med	Low	Med	High	Med-High
Complete Highway Section Replacement	High	High	High	High	Low-Med	High

4 Advanced Selection

4.1 GPR

In 2005, the Minnesota DOT assessed the feasibility of using GPR for a variety of roadway applications and generated a report that indicated GPR was effective for revealing near-surface voids resulting from consolidation and erosion of the base material (Loken, 2005). Other studies have established GPR as a means for detecting void formation beneath asphalt and concrete overlays (e.g., Hauser, 2002) as well as void formation around leaking utilities (Lewis, 2002). While field validation success is an indicator of effectiveness, other GPR attributes are relevant to the additional evaluation criteria:

Feasibility – GPR is a commercially available system. Several geophysical companies offer off-the-shelf equipment for performing subsurface characterization. GPR systems are easily transportable and often only one operator is required for data acquisition.

Invasiveness - GPR is completely non-invasive since the radiated low-power RF energy has no impact on the structural integrity of the device under interrogation. Commercial systems are also FCC compliant.

Efficiency – GPR is one of the most efficient characterization methods. Highway-speed (55 mph) deployment is possible with adequate resolution to assess roadway structural

health over a large region (FHWA, 2001). Correlation of multiple GPR transects will yield a high resolution (0.25ft x 1ft x 0.1ft, Length x Width x Depth) volume image in a relatively short period of time.

4.2 CCR

Resistivity surveying was another promising method for void detection. Several studies have validated resistivity characterization as an effective means for mapping subsurface anomalies. The Central Federal Lands Highway Division (CFLHD) commissioned a study to evaluate resistivity techniques for locating and characterizing the extent of subsurface voids formed by lava flows. Field tests showed that a capacitively coupled resistivity system could indicate large, deep (>15 ft) lava tubes as regions of high resistivity (Meglich, 2003). Other studies have demonstrated excellent correlation between resistivity values obtained from CCR surveys to values obtained by more conventional galvanic systems (Pellerin, 1997). Moisture content estimations from CCR data have also shown good correlation to Time Domain Reflectometry (TDR) soil moisture values (Walker, 2002). In addition to enabling rapid surveying, CCR systems can operate in highly resistive environments where galvanic resistivity systems cannot establish sufficient electrical contact with the ground (Doll, 2000). Other performance relevant attributes include:

Feasibility – Commercial CCR systems are readily available (e.g., Geometrics OhmMapper) and require only a single operator for setup and data acquisition.

Invasiveness – CCR is non-invasive. No galvanic coupling is required—conventional resistivity systems require electrode penetration of the surface. CCR dipoles are surface-laid and couple current into the ground without physical penetration.

Efficiency – CCR arrays are towed along the surface and typical advance rates are 0.5-1mph (for 3 ft sampling resolution). These advance rates are much higher than galvanic resistivity systems that require repeated electrode placement in the survey region.

4.3 FWD

Falling weight deflectometry is a standardized method for evaluating pavement structural health. While FWD surveying is often used to estimate subgrade modulus and pavement stiffness to establish appropriate rehabilitation strategies (Hanna, 2002; IDOT, 2005), studies have shown its relevance to void detection. Malvar et al. (2000) demonstrated the effective application of FWD for detection of voids beneath airfields. Malvar showed a correlation between the deflection basin (spatial response) of the impact load and the depth of the void location. The Missouri DOT Research Development and Technology (MoDOT RDT) division conducted an FWD survey of over 200 PCC joints at 27 bridges. The results from this study established FWD as an effective technique for detecting voids under PCC slabs (MoDOT, 2004). In addition to demonstrating proven application relevance, FWD has several operational features that make it a good candidate for void detection and subsidence characterization surveys:

Feasibility – FWD performance is not limited by environmental constraints and the system can be employed in a variety of conditions. High soil moisture and high soil conductivity, which can limit the range and effectiveness of electromagnetic methods, do not affect FWD operation.

Invasiveness – FWD is minimally invasive. While this method does require surface loading, the impact is typically no greater than standard traffic loading.

Efficiency – FWD requires several drops at each location, thus limiting advance rates; however, setup at each sample point is minimal and sampling resolution can be extended to 5-10ft for large surveys.

4.4 Other Methods

Seismic surveys have also demonstrated value for characterizing subsidence conditions. Miller (2002) employed a seismic reflection methodology to image deep dissolution features resulting in the formation of a roadside sinkhole. Seismic refraction tomography is a legitimate method for resolving karst (voids formed by dissolution of soluble rocks) features resulting in cavity formation (Sheehan, 2005). While numerous sources have validated seismic techniques for void detection applications, the prohibitive data acquisition requirements, processing time, and cost associated with seismic surveys did not meet our efficiency and feasibility requirements.

We deemed the other methods listed in Table 1 unsuitable for field evaluations. These methods did not possess certain attributes required by our evaluation criteria. Cross-hole and tomographic methods lack the data acquisition efficiency required for large surveys. Additionally, these methods require penetration of the surface. Electromagnetic Induction (EMI) surveys are non-invasive and can be conducted rapidly; however, they do not offer the resolution or depth sampling to effectively and reliably detect void presence. Infrared surveys are also non-invasive and require minimal sampling time; however, it is likely that infrared detection methods are only effective during thermal transition periods of the day, and at best will only identify anomalies within a few inches of the road surface. Gravity methods require extremely long sampling periods, low-noise environments, and precise elevation measurements to detect anomalies (Mickus, 2004), and therefore, do not meet the efficiency and effectiveness criteria for characterizing roadways.

Subsequent to our down-selection, we proceeded to field evaluations of the three candidate technologies. To further investigate the veracity of these methodologies, we tested their application at two Vermont Roadway sites: Interstate 89 and US Route 7.

5 Site Description

With guidance from the Vermont Agency of Transportation (VTTrans) we performed field testing of the selected geophysical methods at two highway sites. Both sites exhibited subsidence, but the extent of settlement and the dissimilar histories of the two sites provided a diverse set of test conditions.

5.1 I-89 Hartford

We collected data over an 800 ft segment in the southbound lane of I-89 between the I-91 junction and the New Hampshire border (Figure 5.1). The approximate location of the “patch area” was between mile marker 0.1 and 0.2, N43°-38’-10.4”, W72°-19’-55.4”

Daily average traffic rates at the nearby junction of I-91 and I-89 are among the highest in the eastern part of the state and thus, daylight working conditions presented some unique challenges. Original construction of the subgrade and subbase layers was completed in the 1950’s; however we did find the material construction specifications and we have surmised that the majority of fill material was derived from the rock cut sections in the connecting ramps on the south side of the I-89/I-91 interchange. Anecdotal information by a longtime employee indicated that fine material may have been placed coincident with the blasted rock.

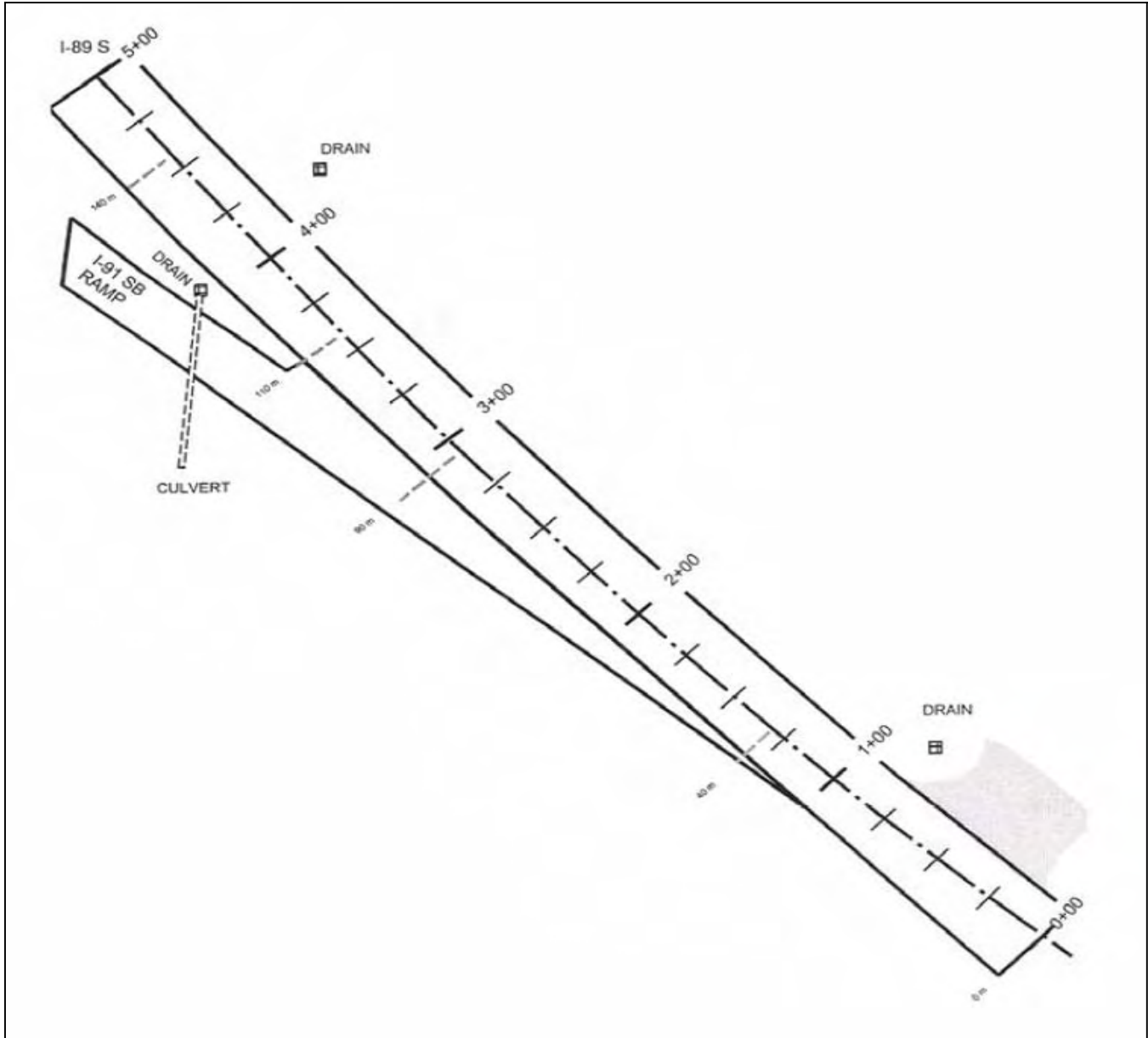


Figure 5.1 Interstate 89 survey site.

Subsidence has been noticed since the early 1980's and according to the maintenance staff has continued steadily during the warm months in recent years. Consistent shimming of the wearing surface has occurred at the site and in 2006 the area required three re-surfacing jobs (Figure 5.2). The slow rate of settlement has made continual patching of the asphalt surface an effective temporary remedy; however, the heavy traffic use of this location and concerns of possible sinkhole formation have established this site as a high priority for evaluation.

The surface drainage control from the highway consists of grated drains in a paved median strip. No curb boards or subsurface strip drainage exists along the immediate shoulder areas. Sink holes of 12-18" diameter were observed on the highway side slope that faces south with one hole near the guard rails and others were seen further down the slope.



Figure 5.2 Interstate 89, Hartford, Vermont looking east toward New Hampshire. The asphalt patch extending across both southbound lanes indicates the region of subsidence.

The greatest settlement occurs in the driving (right hand) lane of the southbound side with some extension into the passing lane. The main portion of the dip extends approximately 100 feet along the driving lane and maximum settlement is close to 3 feet, leaving the original pavement structure altered by thick sections of asphalt overlay.

5.2 US-7 Manchester

The project site is located 0.6 miles north of the Manchester exit on US 7 with the middle of the subsidence area at N43°-10'-50.3", W73°-01'-22.5" (Figure 5.3).

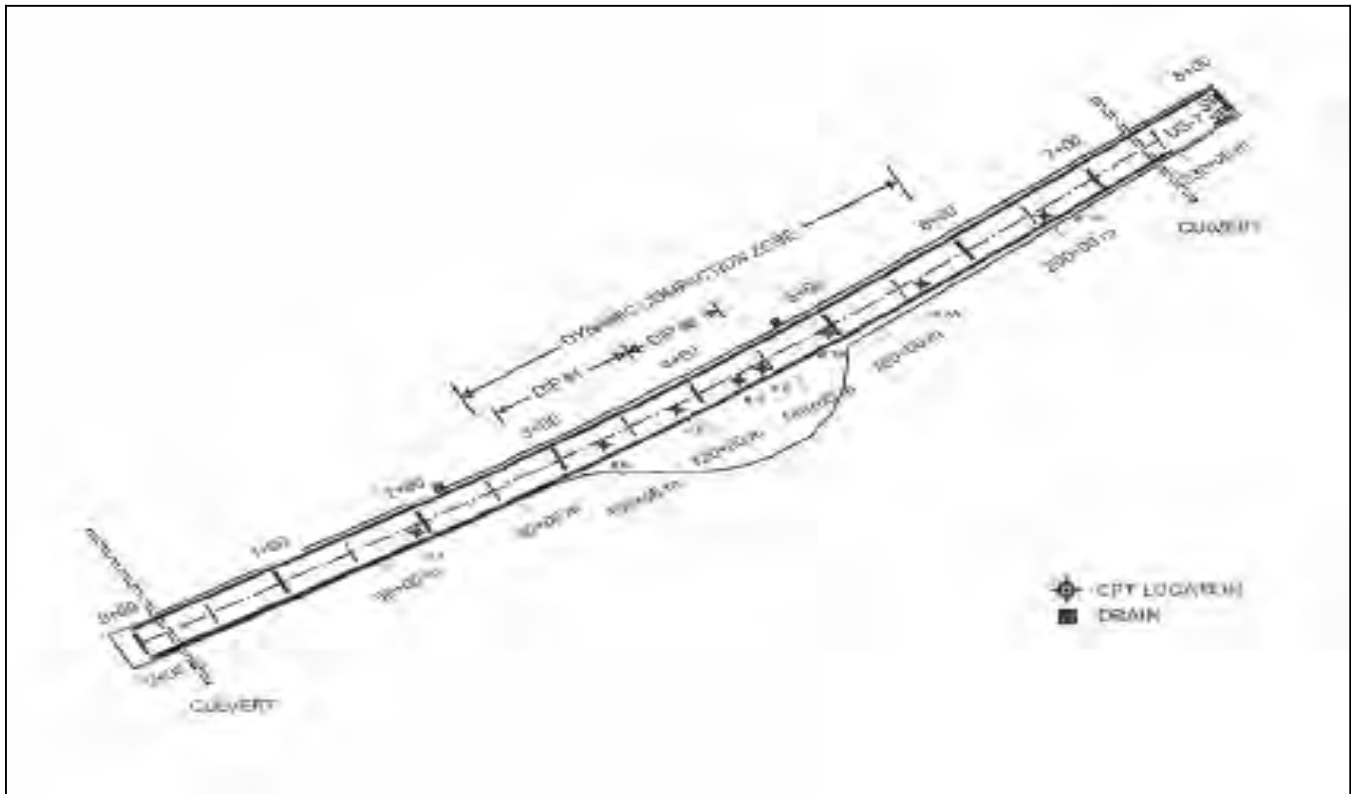


Figure 5.3 US 7 survey site.

The new US-7, called US-7 bypass, was constructed in the early 1990's and the section under study was placed over a dynamically compacted subgrade because the highway passed over a former town landfill. In the last five years, two dips (approximately 85 ft in length from crest to crest) have formed across both travel lanes and shoulders (Figure 5.4). The dips have settled a maximum of 3-4 inches and there had been no re-surfacing to fill the dips at the time of testing. Thus, the original pavement structure was intact for our data collection.

Surface drainage is provided by shoulder curbs and grated drains in the southbound shoulder at two locations along the study site.

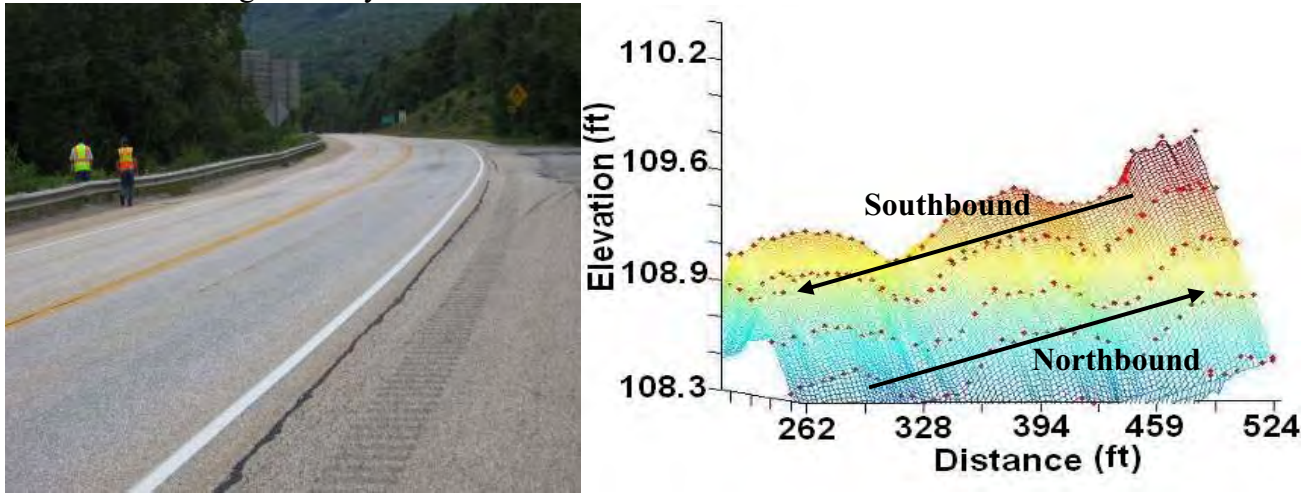


Figure 5.4 (a) Photograph of US Route 7, Manchester, Vermont looking north. Two dips formed across both lanes. (b) Elevation profile map of dips. Dotted lines indicate surveyed points.

6 Data Collection

6.1 Equipment

GPR: We selected GSSI radar antennas with 200, 400, and 900 MHz center frequencies and a GSSI SIR 3000 controller. This range of frequencies provided varying compromises between depth of penetration and range/object resolution. The 400 and 900 MHz antennas were cart-mounted, enabling spatial triggering from the road wheel with resolutions to 0.1-0.2 ft over 100 feet with depth penetrations of roughly 12 ft and 7 ft, respectively. We dragged the larger 200-MHz antenna on a radar-transparent sled with an approximate resolution of 0.5 ft within 100 ft with a depth penetration of roughly 15 ft. This process required a relatively constant advance rate to correlate the temporal triggering with equal length along-track sampling bins.

CCR: We performed resistivity surveys using a Geometrics OhmMapper towed array with a single transmitter and dual receiver configuration. The dipole transmitter capacitively couples current into the ground at the VLF range. Oppositely charged dipole cables are separated from the ground with a thin dielectric sheath. As the transmitter cables are charged with a low frequency AC voltage, the receiver dipoles measure potential gradients in the ground resulting from the capacitive system. The depth associated with each measured resistivity value is a function of the dipole cable lengths and the separation distance between the receivers and the transmitter.

FWD: We collected deflectometer measurements with a Dynatest® towable FWD system operated by the VTrans personnel. We selected three drop heights to provide variable loading to the

pavement surface. An array of geophones recorded corresponding surface deflections at locations radially unique to the loading plate. Figure 6.1 shows the three systems we selected. We also performed a trial survey with a rolling wheel deflectometer (RWD) at the I-89 site using a 53-foot tractor trailer rig outfitted with optical sensors to measure deflections.

CPT: The cone penetrometer testing was accomplished using a tracked 25 ton rig at the I-89 site and a 25 ton wheel mounted unit for the US-7 site. A “standard” cone of 1.75 inch diameter was used for all tests where we measured tip pressure, side friction, and pore pressure. Soil resistivity and soil dielectric properties were measured in some locations. CPT measurements were also converted to SPT blow count using the method of Lunne et al. (1997).



Figure 6.1 (a) GSSI cart-mounted GPR. (b) Geometrics OhmMapper CCR towed array. (c) Dynatest® FWD trailer system.

6.2 Techniques

GPR: We spaced parallel (to traffic flow) GPR transects at 3.28 ft. intervals across both traveling lanes and shoulders at each site (Figure 6.2). To ensure optimal resolution of anomalies running parallel to the direction of travel, we completed a grid survey with across-road transects spaced at 6.6 ft. intervals over the entire survey region; however, we anticipated most elongated anomalies (e.g., culverts) to run perpendicular to the road. The survey areas covered the region(s) of subsidence plus sufficient area to provide a representative sample of the unperturbed pavement structure.

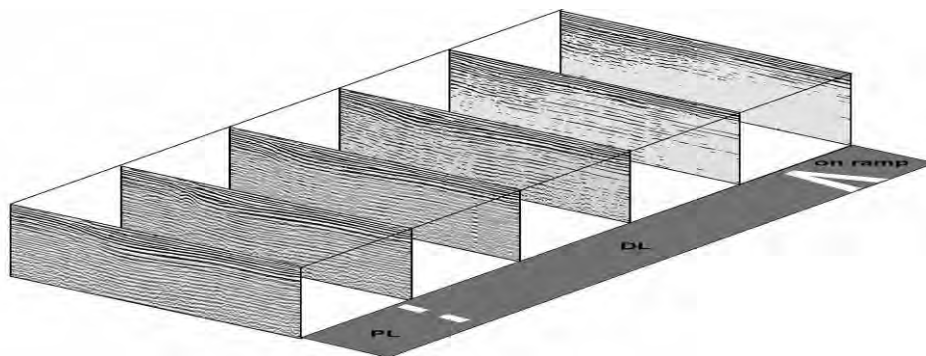


Figure 6.2 Layout of parallel GPR survey transects at I-89 site. Parallel transects were spaced at 3.28 ft intervals. Across-road transects (not shown) were spaced at 6.6 ft intervals.

CCR: Resistivity survey transects overlapped several GPR transects at each of the two sites. We ran parallel transects at 6.6 ft intervals across both travel lanes and shoulders (Figure 6.3). Each transect comprised several passes with different transmit/receive spacings. We acquired most of the transects

using 16.4 ft dipoles; however, we included some 32.8 ft dipole samples to increase the effective depth of interrogation.

FWD: Advance rates were much slower for FWD acquisition than for GPR or CCR surveying. Due to the limited availability of the FWD system and the slow acquisition rates, we selected transects to optimize the information extracted from the FWD survey. At each site, we performed one long parallel transect that covered the area exhibiting the greatest subsidence. We used low resolution (33 ft intervals) sampling to acquire data over the subsidence zone as well as over the undisturbed regions. We collected additional shorter transects at higher resolution (6.6 ft intervals) sampling in the subsidence areas to detect possible highly localized anomalies (i.e., small voids).

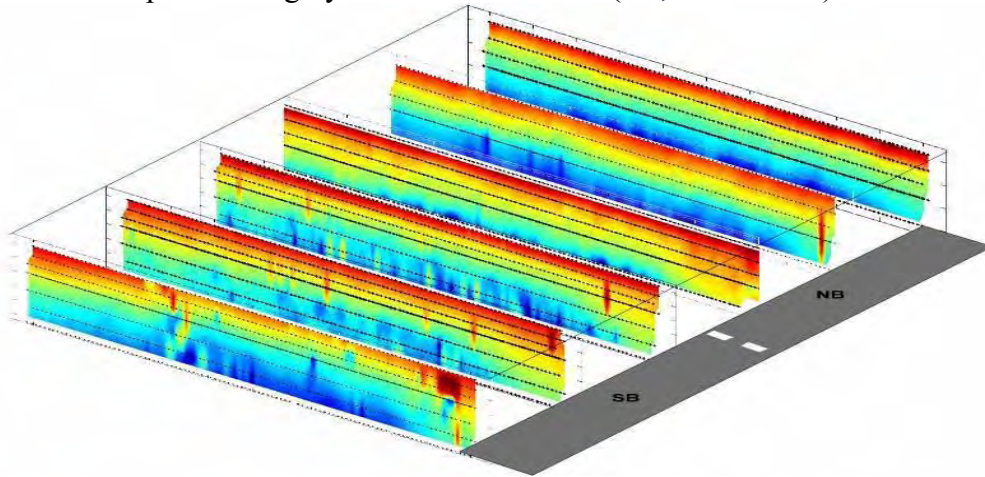


Figure 6.3 Layout of parallel CCR survey transects at US-7 site. Transects were spaced at roughly 6.6 ft intervals.

CPT: For each test a 4" diameter hole was augered through the asphalt pavement (VTrans coring rig) and slightly into the base material with all materials removed. The cone was driven into the base materials hydraulically using the weight of the vehicle to provide the reaction force. The maximum tip pressure the rig could induce was about 12,000 psi and the depth of penetration was allowed to continue until this value was achieved or the onsite engineer indicated sufficient depth had been achieved.

RWD: We performed a single pass over the survey site with the RWD rig to assess correlation between the static and dynamic methods. Results from the RWD test indicate that this may be an excellent method for achieving rapid deflection surveys over large areas. It is likely that the RWD will provide enough sampling resolution to detect and identify large anomalies for further investigation by complementary methods.

7 Site Specific Analysis

7.1 I-89 Hartford

GPR data collected on I-89 revealed the remediation history of the site. Data collected over the asphalt patch showed that the original wearing layer profile had settled to depths of more than 3 ft. in some locations. Years of patching resulted in multiple overlays that were evident in the GPR profiles. The data also indicated the subsidence propagated through the deeper subbase and subgrade layers. The 400-MHz antenna surveys yielded the best results, with sufficient penetration of the patch to resolve small features beneath the overlay. The high attenuation caused by the patch and large transverse cracks associated with the settled base resulted in insufficient penetration with the 900-MHz antenna. While

the 200-MHz antenna provided sufficient depth penetration, it was not able to adequately resolve anomalies of interest beneath the patch. The 400 MHz antenna provided enough penetration and resolution to identify clusters of small wide-angle reflectors beneath the region of greatest subsidence (Figure 7.1).

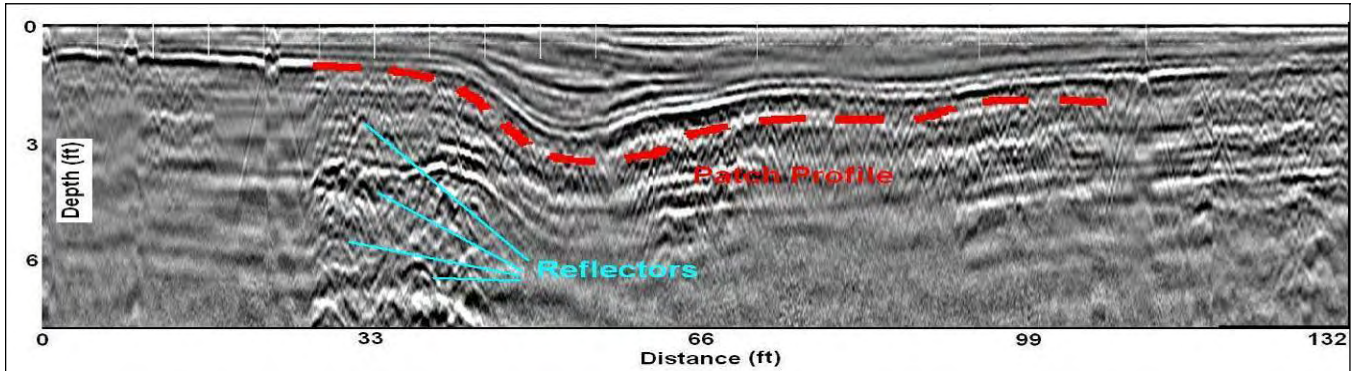


Figure 7.1 400-MHz GPR data beginning at stationing 131+22. Clusters of small reflectors are shown beneath the asphalt patch.

The asphalt patch dominated the response of the CCR array. The resistivity survey identified the decreased conductivity of the asphalt overlay (relative to the base). CCR data revealed that regions of increased resistivity extended to greater depths in the patch region than in the intact regions. Figure 7.2 shows a pseudosection of the resistivity profile collected over the asphalt patch. We primarily used pseudosections for this analysis as a method for indicating relative changes in profile. While inversion methods provide more accurate depth profiles, the pseudosection is adequate for indicating anomalies associated with relative contrasts in apparent bulk resistivity along a transect.

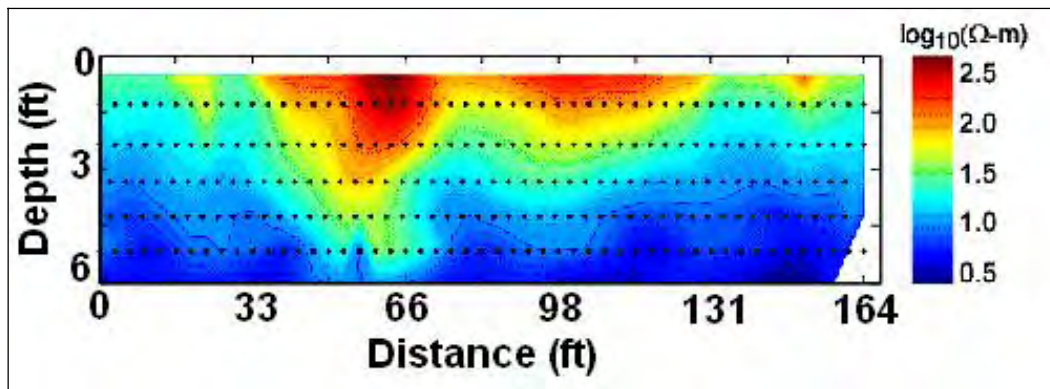


Figure 7.2 Apparent resistivity profile. The asphalt patch is the dominant feature in this pseudosection. The regions of high resistivity (red) correspond to asphalt layers.

Prior remediation at this site increased the difficulty of interpreting the FWD data. The variable thickness of the patch dominated the deflection response of the system, obscuring the signature of small anomalies. The spatial derivative along each transect of the asphalt layer thickness profile was too large for back-calculation of layer moduli using a standard deflection basin fit analysis, which assumes a uniform layer thickness (spatial derivative equal to zero).

While the FWD data were difficult to interpret, we did find good correlation between the static FWD tests and our dynamic deflection tests using the RWD rig. Figure 7.3 shows the correlation between the RWD and FWD tests.

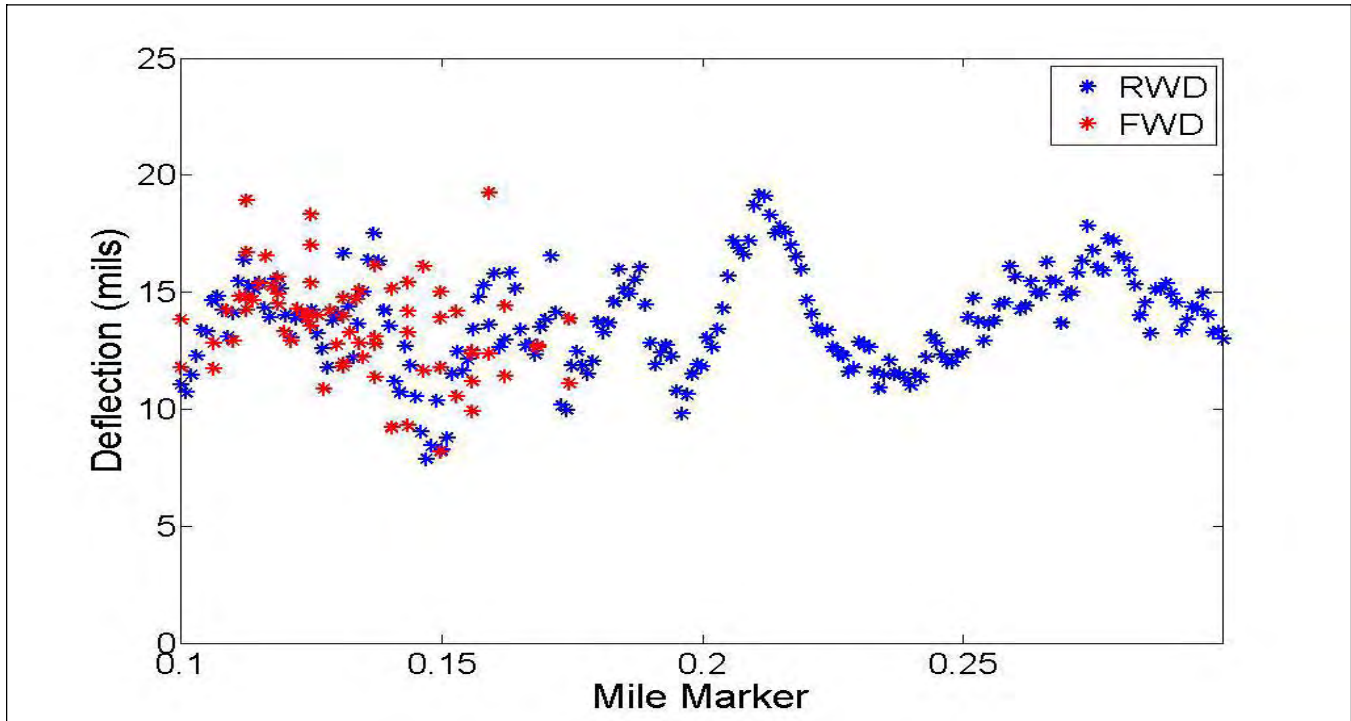


Figure 7.3 Deflection values generated from RWD (blue) measurements and FWD (red) measurements.

7.2 US-7 Manchester

As a result of the experience on I-89, we concluded that 400-MHz data would provide sufficient resolution of subsurface anomalies (we did not collect 900-MHz data at the US-7 site). Both 200-MHz and 400-MHz GPR data collected on US-7 revealed a strong correlation between regions of high signal attenuation and regions of subsidence. Significant signal loss occurred beneath the subbase layer in the two subsidence zones. Our processing steps included background subtraction, infinite impulse response (IIR) filtering, and depth gain; however, the “washed out” appearance in the attenuation zones was clearly evident in the raw data.

Additionally, profiles returned in both data sets indicated a layer corresponding to the original ground profile. Construction of this section of highway required large volumes of fill to create a level base surface. We were able to correlate features of the subgrade profile (dotted blue line in Figure 7.4) shown in GPR data to historical ground elevation data (solid red line in Figure 7.4) collected in a pre-construction survey. We obtained depth scales for the GPR profiles by correlating the two-way travel time of returns from the culvert to its known depth at the northern end of the project site.

CCR data at this site show a strong correlation of lower resistivity (higher conductivity) values to the subsidence regions (Figure 7.4). Depth profiles reveal a noticeable decrease in resistivity beneath both dips. These decreased values also correspond to the regions of high GPR attenuation.

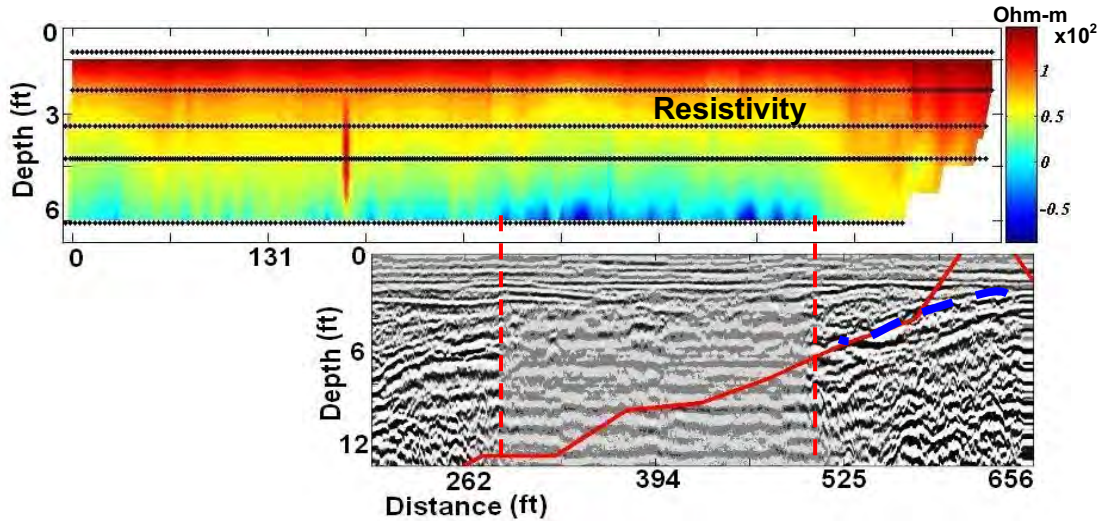


Figure 7.4 Correlated GPR and CCR data. Dotted red lines correspond to subsidence zone. GPR data are “washed out” due to attenuation in this region. The solid red line is the original ground elevation at the site. The dotted blue line traces the subgrade layer shown in the GPR profile.

Deflectometer data correlate higher deflection values with the two dips. Figure 7.5 aligns the road surface profile along the dips with the corresponding peak deflection values at each FWD loading plate sample point (both high resolution and low resolution transects shown). A spike in the deflection data occurs at the transition to each dip. These spikes result from surface crack formation at each of these transitions.

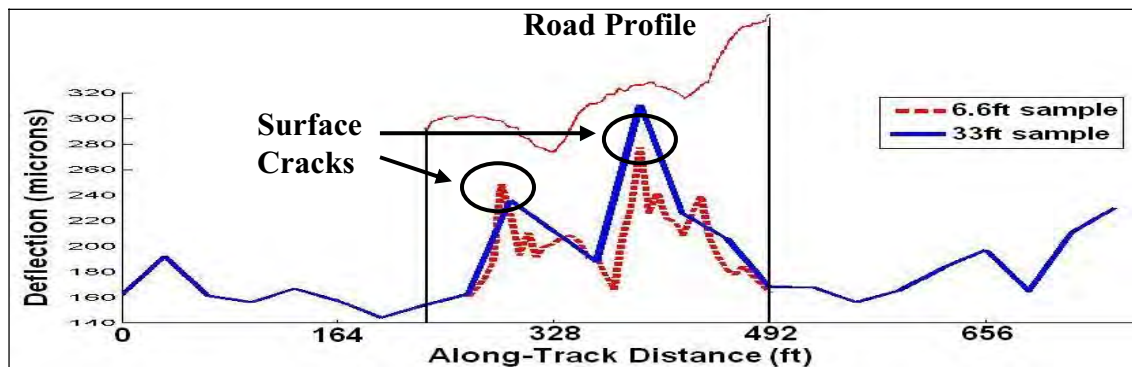


Figure 7.5 FWD deflection profiles show increased values over dips. Deflection peaks correspond to surface cracks close to the dips.

Because of the uniform pavement structure, we were able to use GPR data to determine layer thickness for back-calculation of modulus values. We grouped the structure into three layers: asphalt/base, subbase, and subgrade. An analysis of the deflection basin (deflections at each geophone) data and the corresponding layer thickness values provided the layer moduli. We used the Dynatest® ELMOD5 software to perform the back calculation. The modulus profiles show a sharp increase in the subgrade stiffness at one edge of the subsidence zone (Figure 7.6).

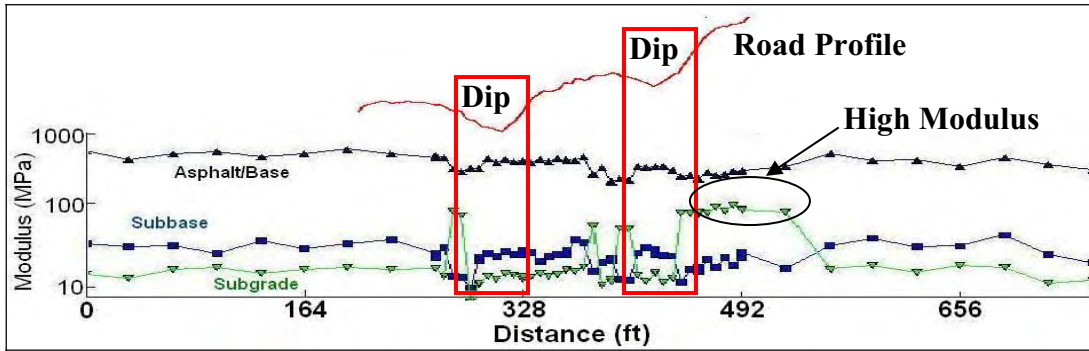


Figure 7.6 Layer modulus profiles. The subgrade modulus increases just after the dip locations.

8 Results

8.1 I-89

The thick asphalt overlay accumulated from years of patching this site dominated the returns from our sensors. While it was difficult to extract additional features from the CCR and FWD data, the 400 MHz GPR data provided enough penetration and resolution to identify several small reflectors beneath the patch. The absence of a large region of dielectric mismatch indicates that no major void is present at this site; however, the number of reflectors permeating the subgrade suggests the existence of small voids (~2-4 in) throughout the substructure.

To augment our understanding of the subsidence processes at this site, we selected several locations for boring and cone penetrometer testing (CPT). After boring through the asphalt layer at each location, our 20-ton CPT rig pushed cone probes through the subbase and subgrade. We selected probes to measure effective blow count (total sleeve and tip resistance), tip pressure (tip resistance), and sleeve/tip ratio (sleeve resistance to tip resistance ratio). These three metrics provide an indication of soil impedance at depths.

The cone penetrometer testing was performed approximately 2 months after the GPR and CCR surveys. The following table identifies the location of auger and CPT data taken in the southbound lane of I-89 near the intersection with the I-91 off ramp.

Table 3: CPT locations, I-89 Southbound Lane, 23 August 2007

Location	ARA Stationing (ft)	ARA Stationing (m)	~VTrans Stationing (ft)	Asphalt Thickness (in)	CPT Data	CPT Depth (ft)
1	3+94, 13.1L	120, 4L	18+28	7	Yes	4.1
2	3+79, 3.3R	115.5, 1R	18+14	10	Yes	2.8
3	2+27, 3.3R	69.3, 1R	16+62	23	Yes	4.1
4	2+00, 3.3R	61, 1R	16+35	36	Yes	21.2
5	1+96, 3.3R	59.6, 1R	16+30	34	Yes	15.6
6	1+80, 3.3R	55, 1R	16+15	13		
6A	0+75, 3.3R	23, 1R	15+10	8.5		
7	1+80, 3.3L	55, 1L	16+15	18		
8	1+94, 3.3L	59, 1L	16+29	25		
9	2+00, 3.3L	61, 1L	16+35	25.5	Yes	6.1
10	2+29, 3.3L	69.9, 1L	16+64	21		

We graphically present CPT data for pushes performed at sites 4 and 5 only, as refusal was encountered at shallow depths below the pavement surface for all the other tests. Both locations (4 & 5) were relatively close to each other (within 6 feet) and were deliberately sited in the area of the thickest pavement. The soil descriptions in the sixth column of the CPT figures are based on data correlated with natural in-situ soils and do not characterize the type of soils or materials encountered beneath pavements.

The first two CPT soundings were outside the area of interest in sections that had not been shimmed while the remaining four were within the “patch” area. Refusal was encountered in four of the pushes, including the two outside the “patch area.” The two pushes, #4 & #5 that exceeded 15 ft are included in the data set in appendix C. Tests # 4 and #5 were pushed within 6 feet of each other, yet test #6, also within 6 ft of test #4 hit refusal at a shallow depth of only 5 ft.

Figure 8.1 shows the data over the entire depth of push from the test #4, while figure 8.2 examines only the data from 10-20 ft.

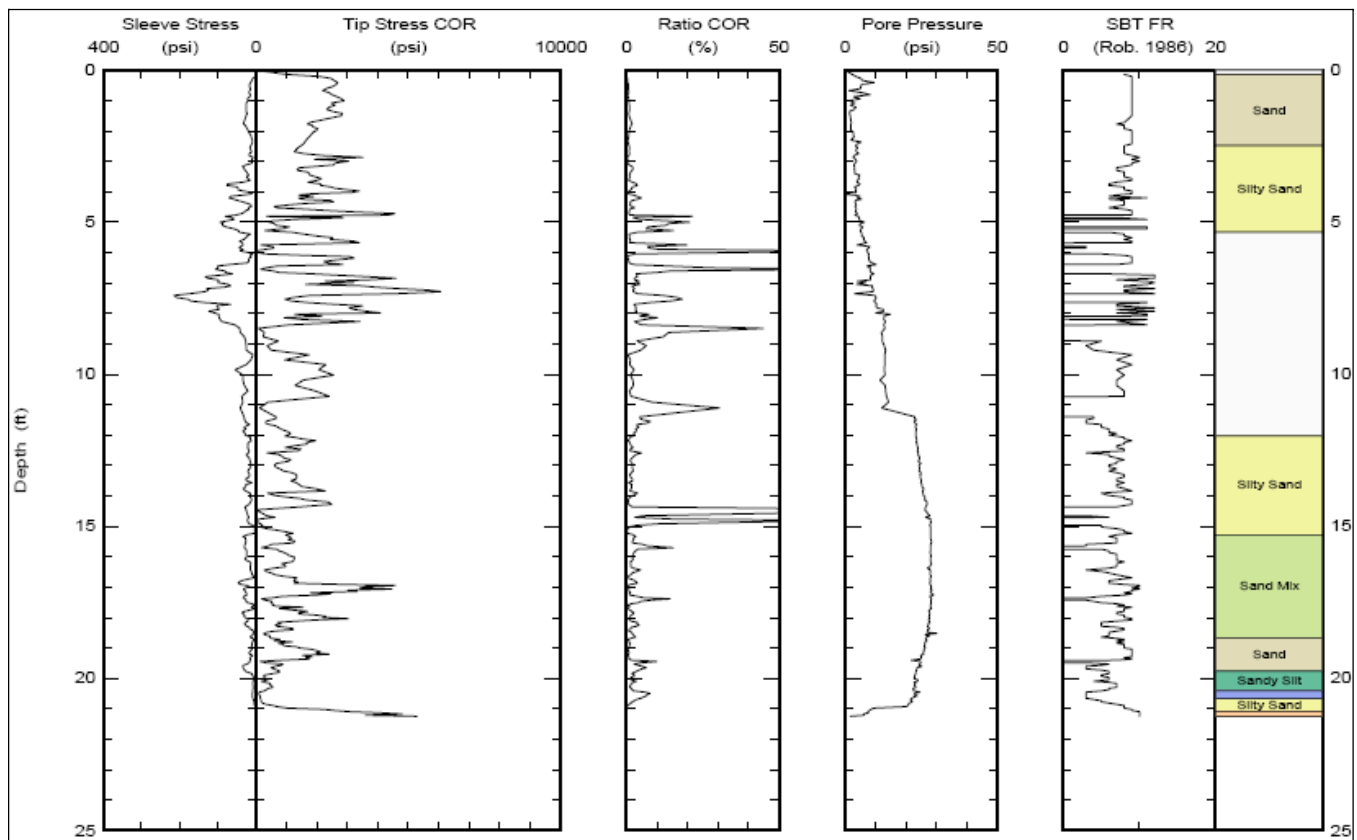


Figure 8.1 Full CPT sounding, test #4.

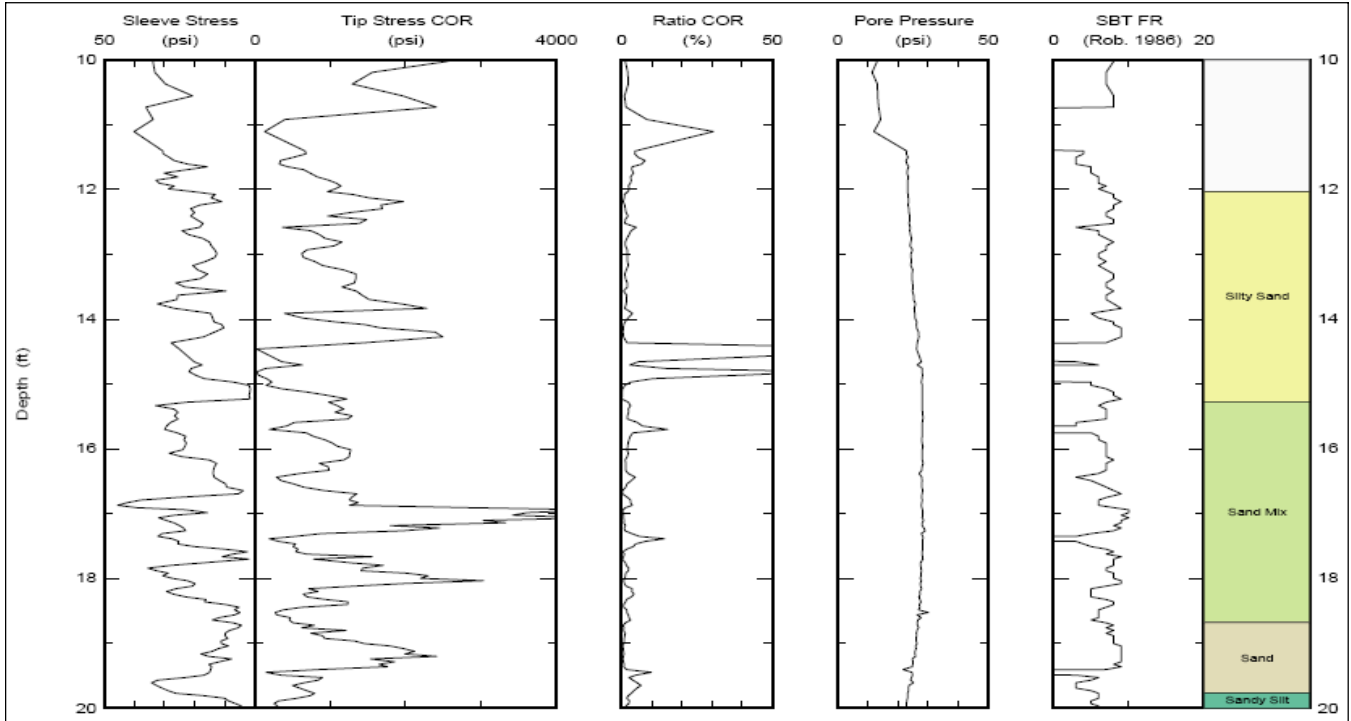


Figure 8.2 Segment of CPT sounding, test #4.

The interesting feature of the CPT data from test #4 is that the cone consistently went from very strong to very weak soil conditions, almost in a regular cyclic pattern from a depth of 14 to 20 ft. Figure 8.3 illustrates the data taken from push #5 and it also shows weak soils beginning at roughly 13 ft, but the cyclic pattern is not as evident as shown in test #4.

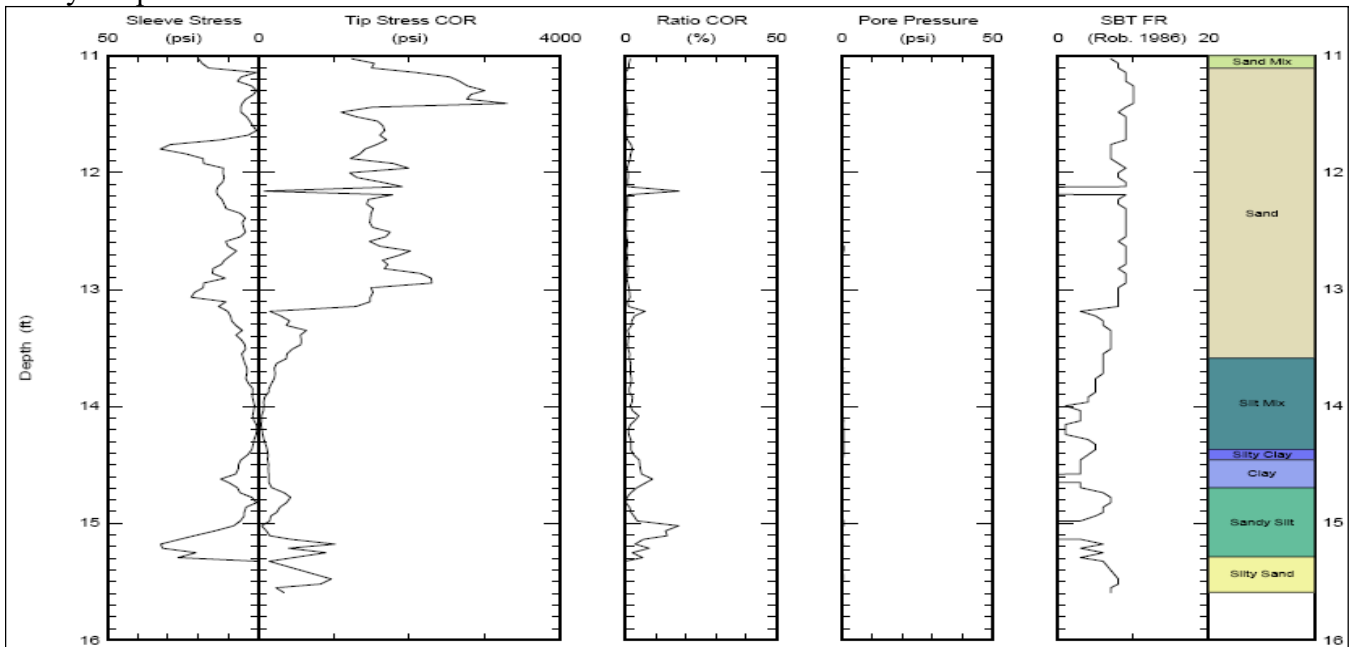


Figure 8.3 Segment of CPT sounding, test #5.

We found a strong correlation between GPR reflectors and low impedance measurements from the penetrometer. CPT data near the asphalt patch showed multiple drops in soil resistance at depths

greater than 6 feet (Figure 8.4a). These drops likely correspond to small void spaces in the subbase and subgrade. Additionally, we were able to obtain some visual confirmation of small void presence from the boreholes generated by CPT collection. The borings revealed a layer of 2-4 in stones mixed into the subbase (Figure 8.4b). Void formation may have occurred around these stones in the subsidence region as a result of fine particle migration. We also found evidence of drainage problems near the subsiding area in the form of an approximately 3 foot wide sinkhole off the shoulder (Figure 8.4c). The drainage issues combined with the subbase composition may have resulted in widespread minor void formation in the pavement substructure.

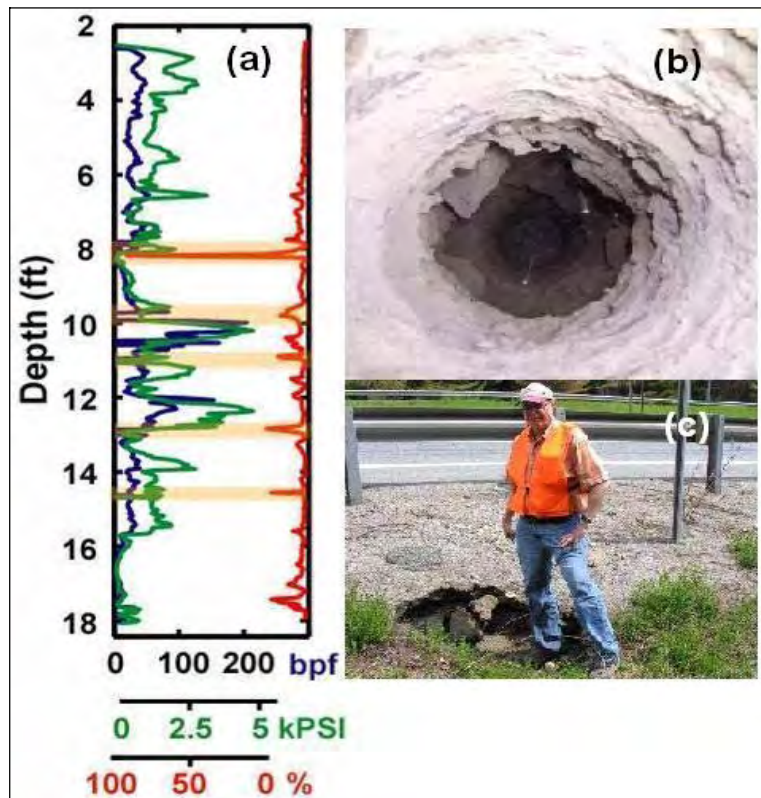


Figure 8.4 (a) CPT profiles. Drops in blow count and tip pressure (blue and green respectively) and spikes in sleeve/tip ratio (red) indicate voids. (b) Borehole showing subbase composition. (c) Sinkhole near the site.

We interpret the GPR, CCR & CPT data and the physical evidence at the site as follows. No large void or voids in the base materials could be detected from the GPR data. The subsidence at the site has been occurring at a slow rate since the construction of the highway in the early 60's and it has accelerated in the last few years with increased shimming of the pavement surface. The slow subsidence is likely being caused by small voids (6-12" diameter size) being formed between the larger rock material in the sub base materials due to water moving through this zone and removing the fines that were used to compact the larger materials. The source of water, based on the physical evidence, appears to be from surface runoff from the pavement through the sink holes that have formed on the side slope of the fill region as well as from infiltration through the many cracks in the pavement.

We opine that the site will continue to subside in a slow but deliberate manner until the water source can be significantly reduced. The subsidence should slow once the majority of infiltrating water can be redirected to proper drainage.

We recommend a two-phase approach to rehabilitate the site, 1) install drainage control and resurface the section to an acceptable grade and observe the pavement deflection with onsite survey measurements over a period of 3-5 years and if this remediation does not work, then 2) onsite grouting should be performed over the affected locations at depths from 13-20 ft; probably over a 100 ft section of roadway, including both lanes and the on ramp section.

Vertical grouting from the pavement surface in this area will be difficult due to the heavy traffic; however, temporary lane closures would enable grouting with minimal impact to traffic flow. Directional drilling and grouting from the side slope may be a viable option, but earthwork will be required on the side slope to provide sufficient platform space for a grouting operation. Recommending details of grouting techniques is beyond the scope of the current project.

The mitigation method of base material removal and subsequent replacement was considered, but due to the tight construction space, the heavy traffic load with significant traffic delays and the 20-25 ft depth of material removal, the first estimate of cost seemed excessive and prohibitive at this time.

8.2 US-7

Results from all methods used at this site are strongly correlated. The GPR data show significant attenuation in the subbase under the subsiding portions of road. CCR data reveal decreased resistivity in the same locations. Both high GPR attenuation and decreased resistivity signify increased moisture content in the subsidence zones. Analysis of FWD deflection basins indicates a stiffer subgrade section leading into the subsidence zone. Both GPR profiles and historical survey data show that this section of subgrade slopes downward to the subsidence regions. Figure 8.5 shows a summary of the correlated results from the site data.

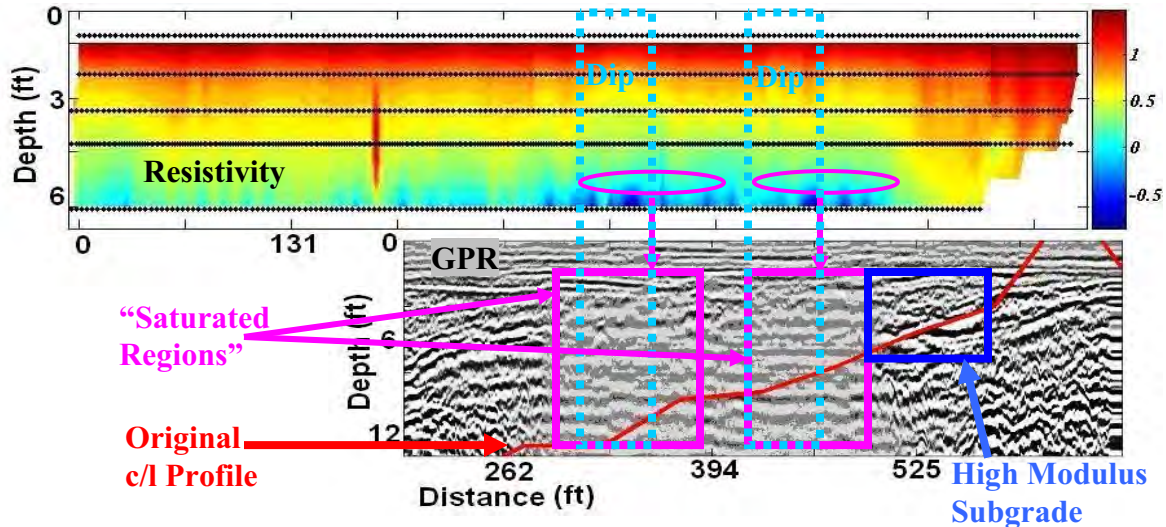


Figure 8.5 Correlation of GPR and CCR data reveal regions of saturation beneath the subsidence zones (dips). The high modulus subgrade (dark blue) corresponds to a compacted base layer that appears to retain water into the saturated zones.

Figures 8.6 and 8.7 below show the 400-MHz and 200-MHz data for a profile run south to north 3.3 ft. left of the centerline. Shown on the figures are the location of the CPT soundings (white vertical lines) and the original ground surface along the highway centerline, (dashed red).

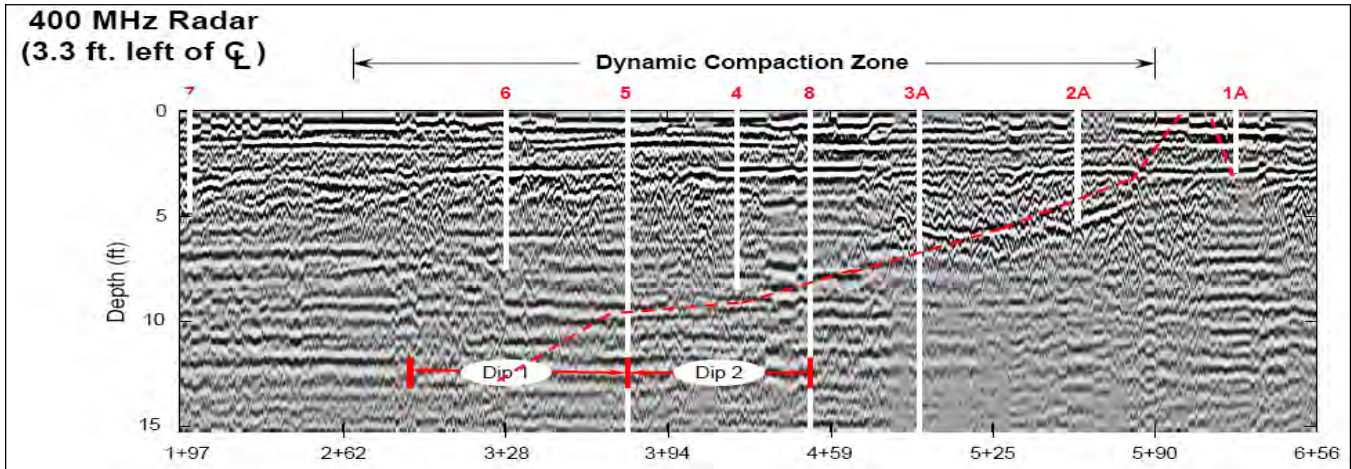


Figure 8.6 400 MHz radar plot with CPT locations.

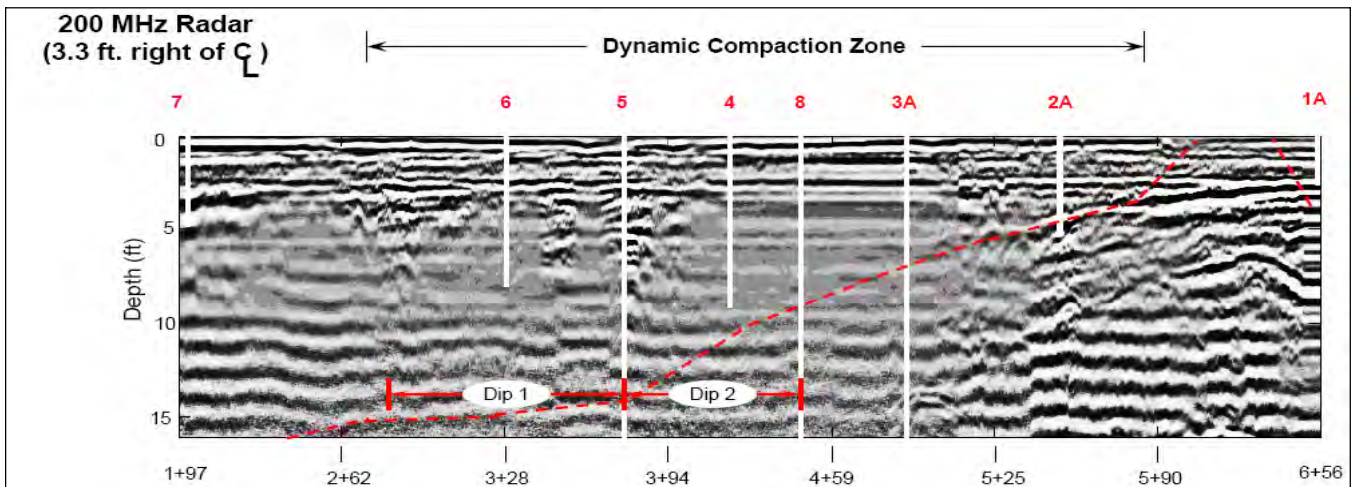


Figure 8.7 200 MHz radar plot with CPT sounding locations.

VTrans provided a truck-mounted rig to auger through the frozen pavement and approximately 1.5 ft of frozen base material. The 25-ton truck mounted CPT aligned the cone penetrometer over each augered hole and advanced the 1.75 in diameter cone to refusal in each hole or until the onsite staff determined that sufficient data had been collected in each hole.

Table 4 CPT locations-US-7 Northbound Lane: Data taken at 3.3 feet off centerline

Loc.	ARA Stationing (ft)	ARA Stationing (m)	~VTrans Local Stationing (ft)	Coring depth (ft)	Asphalt Thickness (ft)	CPT Depth (ft)	Note
1A	6+56	200	13+71	2.4	0.20	4.5	Refusal
2A	5+58	170	12+77	2.3	0.70	6.5	Refusal
3A	4+92	150	12+07	2.5	0.70	18.4	
4	4+27	130	11+42	2.5	0.65	9.2	Refusal
5	3+77	115	10+92	1.9	0.40	17.8	
6	3+28	100	10+43	2.85	0.55	7.7	Refusal
7	1+97	60	9+12	3.1	0.25	5.3	Refusal
8	4+46	136	11+61	3.0	0.55	24.7	

The CPT tests at locations 1A and 7, based on VTrans site plans (No 019-2(1.9)), are outside the area in which dynamic compaction occurred. All other pushes were within the compaction zone. Test 7 also appears to be on the edge of the zone labeled “gravel pit.” The dynamic compaction zone was identified by VTrans as an area of a former refuse dump location. The ARA radar and resistivity surveying began at the VTrans stationing of ~7+15.

A graphical presentation of the CPT for site 5 is given below in Figure 8.8. The data imply relatively strong layers at about 5 and 7 ft, which are also evident in the GPR data; however, at greater depths, the soil strength declines and a very weak soil layer is encountered at 13-16 feet. Beneath this weak layer, the soil strength increases again.

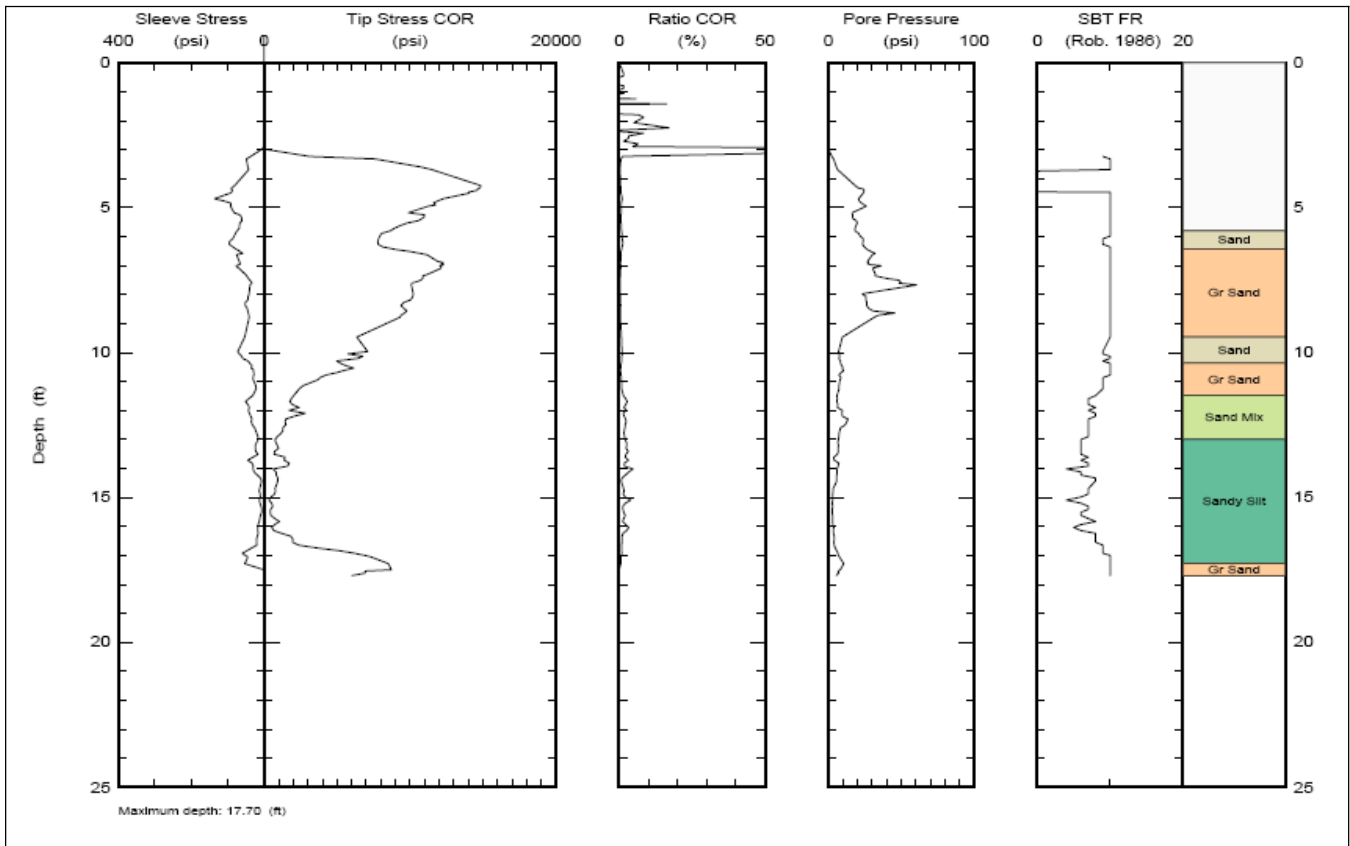


Figure 8.8 CPT sounding at site 5 which is the middle crest between the two dips.

Figure 8.9 shows CPT sounding at site 8, on the outer crest of dip #2. Termination of this push was not due to refusal. The soil strength data is similar to push #5, showing the dynamically compacted zone in the upper 10 ft, but the strength tapers off below and from roughly 13 to 17 feet and again below 20 ft., the soil is extremely weak. CPT sounding #3A also exhibits the same characteristics as the two presented in Figures 8.5 and 8.6, yet this one was outside the dip area.

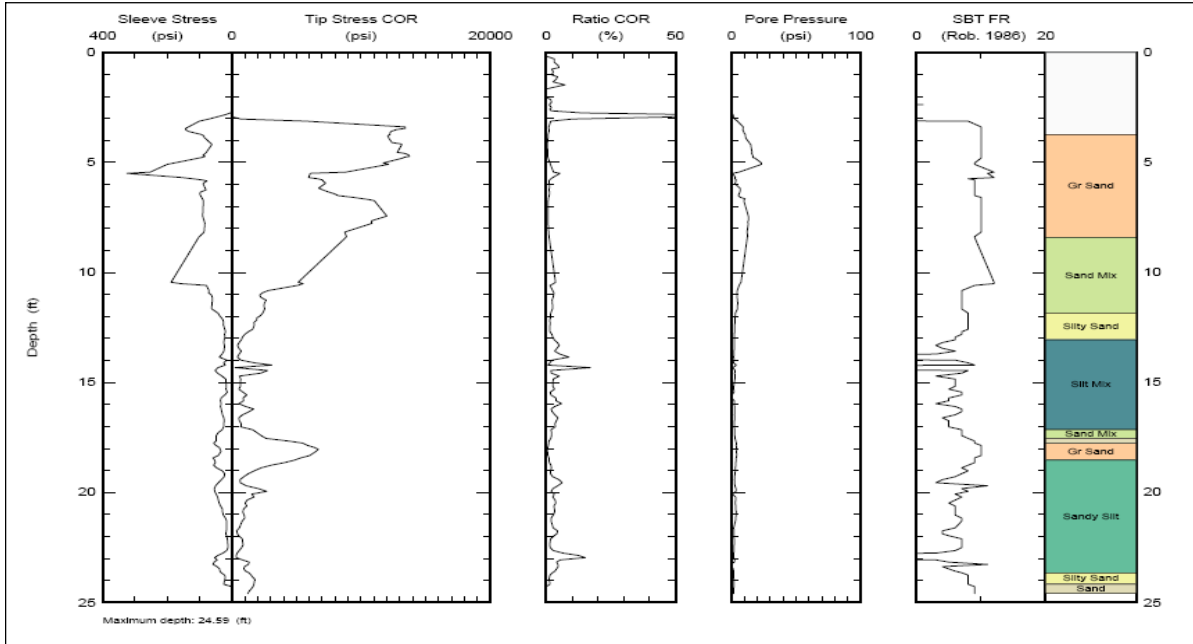


Figure 8.9 CPT sounding at site 8, on the outer crest of dip #2.

The interpretation of the data from the CPT soundings is as follows. The CPT soundings that were able to penetrate the dynamically compacted zone show consistent data, high strength soils in the first 10 ft below the pavement. It is likely the data in Figures 8.8 and 8.9 are representative of the entire area under and on either side of the dips. Both the GPR and CCR show moisture attenuation at a depth of roughly 6-7 ft, and this is confirmed by the rise in the pore pressure in the CPT data for this region. As the soil strength declines, so does the pore pressure, which implies there is not a groundwater problem at the site. As mentioned earlier in the section, the soil classification in the sixth column is not necessarily correct as the scheme was developed for “undisturbed native” soils, not soils that have been disturbed, mixed or compacted into engineered soil materials, or which may include non-geologic materials. Figure 8.10 shows CPT tip pressure traces overlaid on the corresponding 400 MHz GPR transect.

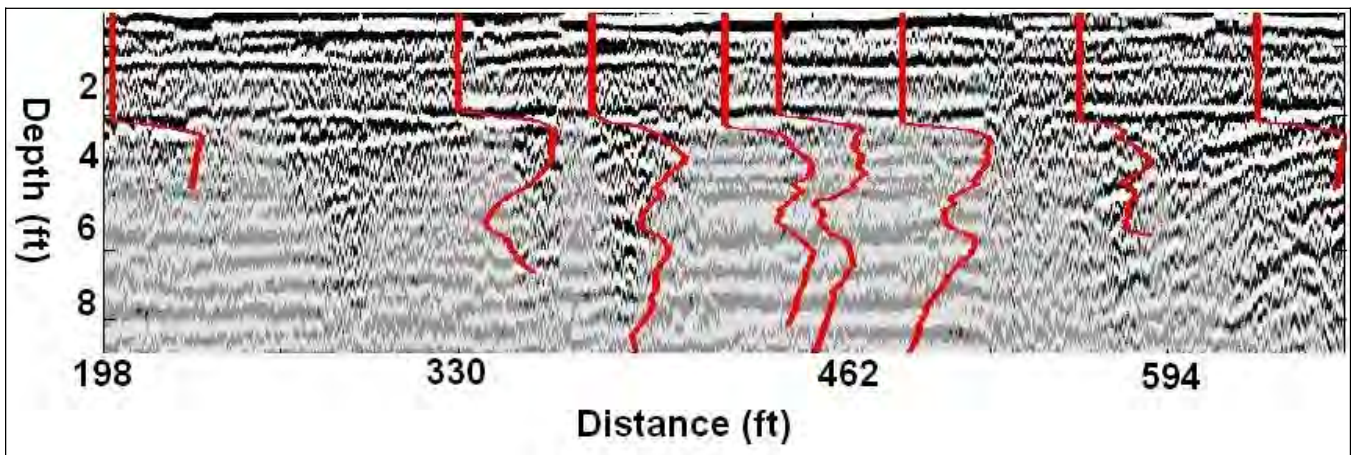


Figure 8.10 400 MHz GPR transect overlaid with CPT tip pressure traces.

CPT data from the subsidence zone show two peaks corresponding to two dynamically compacted layers. It is likely that the drop in tip pressure between the layers is due to inadequate soil compaction. The dynamically compacted layers indicated by the tip pressure peaks in the CPT data also correlate strongly with the fill layers evident in the GPR data. Figure 8.11 illustrates the correlation between these two methods for identifying the structural characteristics of the fill region.

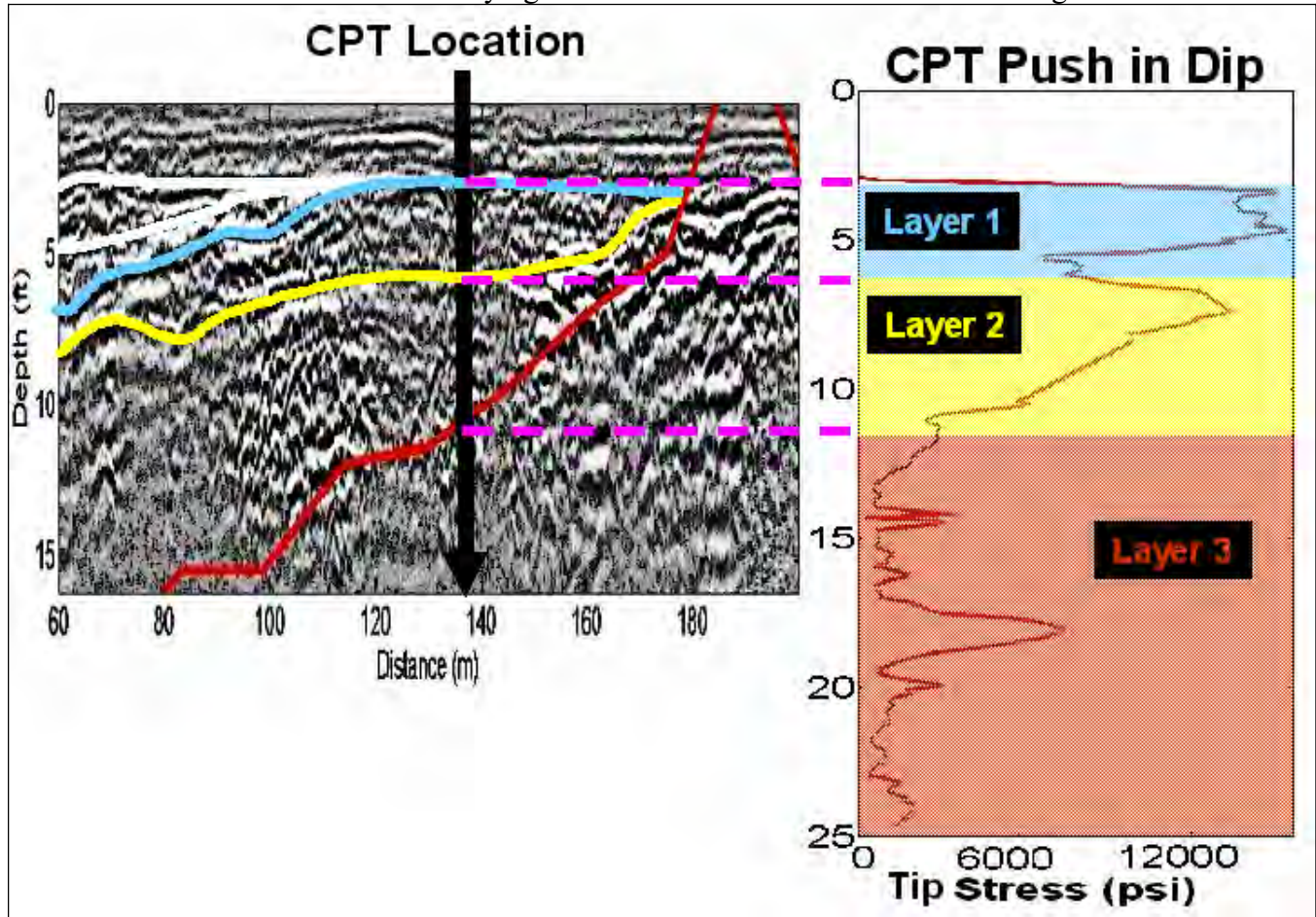


Figure 8.11 Correlation between GPR profile (left) and CPT profile (right). Yellow and blue layers correspond to dynamically compacted fill layers; the red layer corresponds to the original ground layer.

The methods do not suggest the presence of any major voids at this site. Subsidence at US-7 is likely a result of weak materials (either soils or a mixture of refuse) below the dynamically compacted zone and over the years this layer of material has exhibited creep failure. It would appear that the dynamically compacted zone was not sufficiently deep enough or a layer between 13 and 17 ft. was not adequately compacted

The CPT pore pressure data do not indicate that the extremely weak materials are saturated, nor do they appear to be particularly fine-grained. The tip and sleeve pressure signatures are indicative of peat (not likely in a gravel pit) or a non geologic material (land fill refuse), which the standard CPT soil classification schema fail to discriminate.

The mitigation matrix identified in an earlier section is applied to this site (Table 5). It appears from the CPT data that the weak material lies between 13 and 25 ft. There are various options with

respect to the different treatments and to adequately assess them would require further detailed engineering drawings and more information about the site than what is presently available. The complete highway section replacement would require a depth of excavation of roughly 25 ft to replace the weak material; re-routing the traffic through old US-7 would appear to be the only alternative because the depth of material removal is so extreme and a temporary road around the site would likely be cost prohibitive.

The surface treatment does not address the root of the problem and we feel the subsidence will continue regardless of any drainage control. Since the full depth replacement option is too excessive in the quantities of material moved, and routing traffic through Manchester will cause significant congestion in the downtown area, the best option is in-situ soil strength treatment using a grouting technique.

Since we have not been able to correctly identify the weak material (it could be land fill refuse), we recommend that core samples be taken from this layer to properly classify the material between 13 and 25 ft below the pavement surface in the dip area. When the type of material has been properly identified in the weak zone, it will then be possible to recommend the precise grouting technique at the US-7 site.

Table 5 Evaluation matrix for US-7 subsidence

Mitigation Technique	Probability of Long Term Success	Disruption to Traffic	Contractor Availability	Q/A & Durability	Safety of Operations	Costs
Surface Treatments	Low	Low	High	Hi	Hi	Low
In-situ soil strength treatments	Med-High	Low	Med	Med-High	High	Med-High
Complete Highway Section Replacement	High	High	High	High	Low	High

9 Conclusions and Recommendations

9.1 Method Selection

Analyzing a site to determine the extent of subsidence conditions requires a balance of cost-effective and timely measures with thorough and accurate methods. Selection of appropriate investigation methods must rely on several criteria. The most fundamental and crucial gauge of the merit and pertinence of a certain method is its effectiveness—will the technique accurately and reliably characterize the subsurface to the extent necessary for determining structural health? This gauge of effectiveness is based on the general technology maturity and repeated validations of the method in similar applications. Additional selection criteria should focus on the operational attributes and challenges of the technique:

Is employment of the method on a highway *feasible*? Is the equipment readily available and is it easy to transport and set up with limited lane closures? Are the measurements susceptible to traffic noise?

Is the method *invasive*, and if so, to what extent? Will measurements require boring into the pavement surface and will they disrupt the underlying base structure? What level of repair is required to rectify any damages?

Is the method *efficient*? Are advance rates prohibitively low? Will measurements cover a large area with high resolution?

To answer the questions posed by the selection process, one must also consider the constraints of the project. Resource availability and operator training are important factors in determining feasibility of a method. Budget and site use should be considered when estimating an acceptable level of invasiveness. Time constraints and area of coverage are important to assessing the level of efficiency required. Our goal in selecting methods for field testing at the two sites was to choose methods that are widely applicable to heavily used highway locations. GPR, CCR, and FWD are methods that are readily available and non-destructive. They require minimal resources to operate and they can be deployed with minor impact to traffic flow (i.e., temporary single lane closures). Additionally, these methods are moderately to highly efficient, covering large areas in a relatively short amount of time.

Results from our field tests suggest that the methods we selected were successful in characterizing the subsurface to an extent that revealed the structural integrity of the underlying layers. Because our results did not indicate the presence of any large voids or cavities at either site we cannot expound on the benefits of these methodologies for characterizing such anomalies; however, based on the level of detail provided by the sensors, we can assume that such large irregularities would be detected if they occurred within the sensor's effective range. Furthermore, when combined with both knowledge of the site history and the information gleaned from a thorough visual assessment of the surrounding environment, the methods we employed provided us with enough insight to characterize the more difficult small-scale irregularities of the two sites.

Perhaps the greatest asset in using techniques that are conducive to large area assessments is the ability to detect changes from the baseline data. At both highway sites we collected data outside of the problem area to establish baseline characteristics for normal pavement conditions. When the causes of failure are unknown, often the most elucidating assessment is to compare the problem area data to the baseline data rather than to attempt an absolute characterization using the problem area features alone. While baseline comparisons were hindered by the dominant effects of remediation (the asphalt patch) at the I-89 site, they revealed subtle changes at the US-7 site. For example, an analysis of the resistivity profiles shows a distinct decrease in value at the subsidence locations when compared to the baseline. The GPR profiles revealed significant attenuation beneath the subsiding regions. This attenuation appeared as "washout" (loss of structure) in the data when compared to the baseline. These effects would not have been as apparent if we had not referenced the data collected outside the subsidence zones. When the CPT data is used in conjunction with the non-destruction data, a more complete picture of the subsurface conditions unfold.

9.2 Protocol

Once appropriate methods for the site are selected, evaluators should establish a protocol to optimize the techniques and conduct the survey efficiently. Protocol should be developed for two general scenarios: 1) surveys over regions exhibiting deterioration, and 2) surveys over regions that appear intact. Objectives may also influence the protocol. For example an evaluation to merely assess

the risk of catastrophic failure may require a different protocol from an evaluation designed to assess optimal rehabilitation strategies for a failing portion of highway.

Based on our tests conducted at the two sites exhibiting subsidence, we recommend including the following procedures in protocol designed for evaluating regions of known deterioration:

1. Establish a baseline. As described previously, determining the subsurface characteristics of intact regions can yield valuable information when analyzing data collected over deteriorating zones. When non-catastrophic conditions exist (i.e., no large-scale voids are present), subtle deviations from the baseline data can reveal the causes of the problem.
2. Use all the information available. Available information may include site history (e.g., construction materials and procedures), as well as visual information regarding drainage or use patterns. This information can complement the insight gained from data analysis. Corroboration of information leads to greater confidence in interpretations of data. Combining information can be conducted on various levels: from visual correlation of results to the implementation of more sophisticated quantitative fusion methodologies (such as cooperative and joint-inversion of geophysical data).
3. If possible, survey the site prior to any remediation. The condition of a site can greatly impact the effectiveness of any method selected. Our experience with the two sites described in this report has demonstrated that geophysical surveying and analysis may be most effective during the early stages of subsidence—prior to any temporary remediation that may disrupt the pavement structure. Interim treatment of a site can create gross anomalies, masking the features that may be causing the problem. Large-scale voids that could result in catastrophic pavement failure are unlikely to be masked by patching or minor remediation; however, the two sites we surveyed reveal that subsidence can result from processes much more subtle than large void formation.

Surveys targeting large regions of unknown condition may require a slightly different approach from surveys over regions of known failure. While the data analysis will be similar for both types of survey, the operational concept may be different for the larger surveys. We recommend establishing a method or methods for preliminary wide area assessments over large regions of unknown condition. ***Methods selected for wide area assessments should be capable of detecting and identifying anomalies that are indicative of potentially catastrophic failure conditions.*** We recommend two candidate methods for wide area assessments:

1. Based on our experience, GPR is the best candidate for this approach. GPR is an efficient method as it can be deployed from a moving vehicle to rapidly survey vast areas with enough resolution to potentially identify large and catastrophic voids.
2. RWD is useful as a complementary wide area assessment method to GPR because it can provide dynamic measurements of pavement deflection at highway speeds. We have performed a preliminary study that indicates integrating a GPR system with the RWD rig is feasible and practical, but a fully integrated system does not exist at this time.

Regions that are identified as potentially deficient, but do not show any conclusive anomalies may require further investigation. Additional non-destructive methods, such as CCR and FWD, may be used to better understand these regions of interest. While these methods are not as efficient as GPR, they can provide complementary information that will help elucidate non-catastrophic failure modes.

Prior to remediation, invasive ground-truth methods, such as CPT, can be used sparingly to confirm structural deficiencies.

Ultimately, assessing the safety (i.e., imminence of catastrophic failure) of a subsiding road is the most critical milestone in an evaluation. If a road is deemed safe, evaluators should consider the processes causing subsidence, the functionality of the road, and the resources available to repair it when determining the best means of remediation.

9.3 Mitigation

The repair or mitigation of a highway subsidence will depend on many factors including the location on the highway section (including the depth to the problem area), the safety concern in the work zone with respect to vehicular traffic, and ultimately the cost, which reflects all of these factors and others (see the generic table identified in section 4 for a detailed list of factors). The techniques available for mitigation are generally invasive; and the only reliable non-invasive technique found was continued re-surfacing, which would not attack the problem causing the subsidence. Examples of subsidence in typical highways are voids formed from 1) insufficient compaction of the base material, 2) irregular surface grading of the base and the structural pavement, and 3) corrosion of culverts and water/soil infiltration from the subbase materials. Soil particle failures and subsequent movement and consolidation beneath pavements caused by excessive stresses will cause settlement of materials and the entire pavement structure.

It would appear from the analyses at the two sites, that when the failing material or void locations occur at depths greater than 10-12 ft, soil stabilization/strengthening techniques appear as the most logical alternative because of the excessive material removal required for complete highway replacement.

10. References

- Bouillon, A-L., 2005, Geophysics for Geohazards on Land: State-of-the-art, case studies, and education, International Center for Geohazards, ICG Report 2005-T1-1
- Doll, W.E., Gamey, T.J., Nyquist, J.E., Mandell, W., Groom, D., Rhodewald, S., 2000, Evaluation of New Geophysical Tools for Investigation of a Landfill, Camp Roberts, CA, Symposium on Application of Geophysics to Environmental and Engineering Problems (SAGEEP) 2001 Proceedings, Denver, CO
- Federal Highway Administration, 2001, Phenomenology Study of HERMES Ground-Penetrating Radar Technology for Detection and Identification of Common Bridge Deck Features, FHWA-RD-01-090
- Hanna, A.N., Saeed, A., and Hall, J.W., 2002, Determination of Insitu Material Properties of Asphalt Concrete Pavement Layers from Nondestructive Tests, National Cooperative Highway Research Program (NCHRP), Research Results Digest, December 2002 – Number 71
- Hauser, E.C., and Howell, M.J., 2002, Ground Penetrating Radar Survey to Evaluate Roadway Collapse in Northern Ohio, 2001 Symposium on Application of Geophysics to Environmental and Engineering Problems (SAGEEP) 2001 Proceedings, Denver, CO, CD Publication RBA-2
- Illinois Department of Transportation (IDOT), 2005, Pavement Technology Advisory – Non-Destructive Testing with the Falling Weight Deflectometer, Bureau of Materials and Physical Research Report, PTA-T1 (Eff. 10/96, Rev. 02/2005)
- Lewis, J.S., Owen, W.P., and Narwold, C., 2002, GPR as a Tool for Detecting Problems in Highway-Related Construction and Maintenance, 2002 Geophysics Conference, Los Angeles, CA

- Loken, M., 2005, Current State of the Art and Practice of Using GPR for Minnesota Roadway Applications, Minnesota Local Road Research Board Report
- Lunne, T. Robertson, P.K., and McPowell, J.J., 1997, Cone Penetration Testing in Geotechnical Practice, Spon Press, New York, NY, pp. 150-151
- Malvar, L.J., 2000, Issues in Pavement Evaluation, Transportation Systems 2000 (TS2K) Workshop, San Antonio, TX, February 2000 pp.193-202
- Meglich, T.M., Williams, M.C., Hodges, S.M., and DeMarco, M.J., 2003, Subsurface Geophysical Imaging of Lava Tubes, Lava Beds National Monument, CA, Central Federal Lands Highway Division (CFLHD) FHWA Report
- Mickus, K., 2004, The Gravity Method in Engineering and Environmental Applications, Geophysics 2003: Federal Highway Administration and Florida Department of Transportation special publication, in press
- Miller, R.D., 2002, High Resolution Seismic Reflection Investigation of the Subsidence Feature on U.S. Highway 50 at Victory Road Near Hutchinson, Kansas, Kansas Department of Transportation District 5, Report No. 2002-17
- Missouri Department of Transportation, 2004, Void Detection with the Falling Weight Deflectometer, Research Development and Technology Division Investigation 99-044, Report 04-004
- Pellerin, L., Alumbaugh, D.L., and Pfeifer, M.C., 1997, The Electromagnetic Integrated Demonstration at the Idaho National Engineering Laboratory Cold Test Pit, Sandia Corporation Report SAND-97-0904C
- Perrin, J. and C.S. Jhaveri, 2004, The Economic Costs of Culvert Failures, TRB 2004 Annual Meeting, Transportation Research Board
- Sheehan, J.R., Doll, W.E., Watson, D.B., and Mandell, W.A., 2005, Application of Seismic Refraction Tomography to Karst Cavities, U.S. Geological Survey Karst Interest Group Proceedings, Rapid City, South Dakota, September 12-15, 2005, pp. 29-38
- Walker, J. P., and Houser, P.R., 2002, Evaluation of the OhmMapper Instrument for Soil Moisture Measurement, Soil Science Society of America Journal 66:728-734 (2002)